2012

DAMPING OF BOLTED BEAMS WITH UNEQUAL THICKNESS RATIO

Arundhati Pradhan

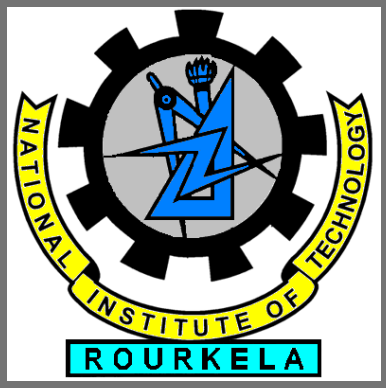

DEPARTMENT OF MECHANICAL ENGINEERING

NATIONAL INSTITUTE OF TECHNOLOGY

ROURKELA - 769008, ODISHA, INDIA

2012

DAMPING OF BOLTED BEAMS WITH UNEQUAL THICKNESS RATIO

A THESIS SUBMITTED IN PARTIAL FULFILLMENT
OF THE REQUIREMENTS FOR THE DEGREE OF
MASTER OF TECHNOLOGY (RES)
IN
MECHANICAL ENGINEERING
BY

ARUNDHATI PRADHAN
610ME301

Under the guidance
of
Prof. Bijoy Kumar Nanda

DEPARTMENT OF MECHANICAL ENGINEERING
NATIONAL INSTITUTE OF TECHNOLOGY
ROURKELA
2012

National Institute of Technology

Rourkela

CERTIFICATE

This is to certify that the thesis entitled, **"DAMPING OF BOLTED BEAMS WITH UNEQUAL THICKNESS RATIO"** submitted by **Mrs. Arundhati Pradhan** in partial fulfillment of the requirements for the award of *Master of Technology (Res)* degree in *Mechanical Engineering* with specialization in *Production Engineering* during session 2010-2012 at the National Institute of Technology, Rourkela (Deemed University) is an authentic work carried out by her under my supervision and guidance. To the best of my knowledge, the matter embodied in the thesis has not been submitted to any other University/Institute for the award of any degree or diploma.

Date:
Rourkela

Prof. B. K. Nanda
Dept. of Mechanical Engg.
National Institute of Technology
Rourkela, Odisha

Acknowledgement

I express my deep sense of gratitude and reverence to my thesis supervisor **Prof. B. K. Nanda**, Professor, Mechanical Engineering Department, National Institute of Technology, Rourkela, for introducing the topic and giving me an opportunity to conduct the present work under his guidance. His invaluable encouragement, helpful suggestions and supervision throughout the course of this work and providing valuable department facilities helped me a lot for the completion of this thesis.

I express my sincere thanks to **Prof. S. K. Sarangi**, Director, NIT, Rourkela for creating healthy working environment in the campus and giving freedom to use the facilities available in the institute for this study.

I would like to thank **Prof. K. P. Maity**, Head of the Department, **Prof. Alok Satapathy** and other faculty and staff members of the department for their help and cooperation for completing the thesis. I would like to thank to **Prof. S. C. Mohanty**, Professor-in-charge of Dynamic Laboratory and his staffs for their cooperation and help in conducting the experiments.

I would also like to thank **Mr. Bhagat Singh** (Ph.D. scholar), **Mr. Srimant Mishra, Miss. Prity Aniva Xess, Mr. Hemanta Kumar Rana** and well-wishers who are involved directly or indirectly in successful completion of the present work.

I would like to thank my parents; my elder Bhaiya and Bhabi for their strong support and encouragement without which the thesis would not have reached the complete stage.

Last but not the least I would like to express thanks to my sweet boy **Bipul** and my husband **Mr. Babrubahan Sahu,** without their support and encouragement this thesis would not have been completed.

(Mrs. Arundhati Pradhan)

ABSTRACT

Rapid development of structural members requiring high damping possesses a big challenge to the designers. An extensive study on the dynamic behaviour of these structures is required in order to assess their damping capacity. This study further helps the designers to know the parameters affecting the dynamic characteristics of these members. Improvement of damping capacity is one of the vital characteristics for these structures. Usually, the structural members have inherently low damping capacity. The damping capacity of a structural member can be enhanced using various techniques such as; inserting visco-elastic layers in between two layers, manufacturing sandwich structures and layered jointed structures. The jointed structures usually provide adequate damping due to micro-slip and friction at the interfaces. Jointed structures are manufactured with the help of fasteners such as bolts, rivets or welds. The bolted structure gives maximum damping compared to the other fasteners. The main source of damping in bolted structures is the energy loss due to friction and micro-slip at the interface of two layers.

The damping capacity of the jointed structures mainly depends upon a number of parameters; length of the beam, thickness ratio, tightening torque on the bolt, and number of layers etc. When a dynamic load is applied on a bolted layered beam, it vibrates with some amplitude of excitation at a particular frequency of vibration and the damping in this type of structure is achieved by the energy dissipation. It is established that 90% of energy dissipation in jointed structure takes place due to micro-slip at the interfaces.

In the present work energy approach has been used to evaluate the damping capacity of structures. Euler-Bernoulli beam theory has been applied as the dimensions of the test specimens satisfy the criterion of thin beam theory. A theoretical equation has been derived to evaluate the damping capacity of the jointed cantilever structures. An experimental set-up has been developed and experiments are conducted with a large number of specimens under different vibrating conditions to authenticate the theory developed. The logarithmic decrement technique has been used for measuring the damping capacity of the structures with the help of a digital storage oscilloscope. The experimental results are compared with the corresponding theoretical ones and useful conclusions have been drawn from both the results accordingly.

Contents

Certificate i
Acknowledgement ii
ABSTRACT iii
Contents iv
List of Tables vi
List of Figures vii
Nomenclature x
1. Introduction **1**

1.1 Background 1
1.2 Motivation 2
1.3 Beam theories 3
1.4 Outlines of the thesis 3
2. Literature review **5**

2.1. Introduction 5
2.2. Vibration and damping 5
2.2.1 Material damping 6
2.2.2 Structural damping 6
2.2.3 Fluid damping 6
2.3. Measurement of structural damping 6
2.3.1. Logarithmic decrement 7
2.3.2. Damping ratio 7
2.3.3. Specific damping capacity (ψ) 8
2.4. Improvement of damping capacity of structures 8
2.4.1. Use of unconstrained and constrained viscoelastic layers 8
2.4.1.1. Unconstrained layer or external damping 8
2.4.1.2. Constrained layer damping 9
2.4.2. Use of special high damping inserts 10
2.4.3. Use of layered and jointed constructions 10
2.5 Review of literature on jointed structures 10
3. Theoretical analysis by classical energy approach **15**

3.1. Introduction 15
3.2. Dynamic equations of free transverse vibration 16
3.2.1. Evaluation of Constants A_1, A_2, A_3 and A_4 18
3.2.2. Evaluation of Constants A_5 and A_6 20
3.3. Mechanism of micro slip 21
3.3.1. Determination of relative dynamic slip 21
3.4. Theoretical analysis for beam with non-uniform pressure distribution at the interfaces 23
3.4.1. Pressure distribution at the jointed interfaces 23
3.4.1.1. Determination of Non-uniform pressure distribution at the interface 24

3.4.2. Energy dissipation due to friction and micro slip 27
Determination of energy dissipation per cycle of vibration for non-uniform pressure distribution 27
3.4.3. Determination of logarithmic decrement (δ) 29
3.4.3.1. Logarithmic decrement (δ) for non-uniform pressure 30
3.4.4. Determination of product of μα 31
3.5 Theoretical analysis for bolted beam with uniform pressure distribution at the interfaces 31
3.5.1 Determination of Uniform pressure distribution at the interface 31
3.5.2 Determination of energy dissipation per cycle of vibration for uniform pressure distribution 33
3.5.3 Logarithmic decrement (δ) for uniform pressure 34
3.5.4 Determination of product of μα 34
3.6 Chapter summary 35
4. Experimental analysis **36**
4.1. Introduction 36
4.2. Preparation of specimens 36
4.3. Description of the experimental set-up 40
4.4. Testing procedure 46
4.4.1. Measurement of young's modulus of elasticity 46
4.4.2. Measurement of static bending stiffness 46
4.4.3. Measurement of logarithmic damping decrement (δ) 47
4.5. Experimental evaluation of μα 48
4.6. Chapter summary 52
5. Results and Discussion **53**
6. Conclusions and Scope for further research work **65**
Reference **67**
Curriculum Vitae **72**

LIST OF TABLES

3.1	Values of constants in pressure distribution function	25
3.2	Distance between the centers of two consecutive bolts at different thickness ratios for non-uniform pressure at the interfaces	25
3.3	Distance between the centers of two consecutive bolts at different thickness ratios for uniform pressure at the interfaces	32
4.1	Details of mild steel bolted specimens for non-uniform pressure with thickness ratio 1.0	37
4.2	Details of mild steel bolted specimens for non-uniform pressure with thickness ratio 1.5	38
4.3	Details of mild steel bolted specimens for non-uniform pressure with thickness ratio 2.0	38
4.4	Details of mild steel bolted two layers specimens for uniform pressure with thickness ratio 1.0	39
4.5	Details of mild steel bolted multi layered specimens for uniform pressure with thickness ratio 1.0	39
4.6	Details of mild steel bolted specimens for uniform pressure with thickness ratio 1.5	40
4.7	Details of mild steel bolted specimens for uniform pressure with thickness ratio 2.0	40

LIST OF FIGURES

Fig 2.1	Free vibration damping system	7
Fig 2.2	An un-constrained-layer damping system	9
Fig 2.3	A constrained-layer damping system	9
Fig 3.1	Free transverse vibration of a beam	16
Fig 3.2	Mechanism of dynamic slip at the interfaces	22
Fig 3.3	Free body diagram of a bolted joint showing the parabolic influence zone	23
Fig 3.4	Variation of Pressure distribution (P/σ_s) for different thickness ratio at different distance (R/R_B)	25
Fig 3.5	Influence area under the bolt head	26
Fig 3.6	Relationship between the frictional force (F_r)and relative dynamic slip(u_r) during one cycle.	28
Fig 3.7	Uniform pressure distribution of bolted joints by reducing the distance between consecutive bolts	31
Fig 4.1	Two layered mild steel bolted test specimen	37
Fig 4.2	Four layered mild steel bolted test specimen	37
Fig 4.3	Schematic of the experimental set-up	41
Fig 4.4	Photographic view of the experimental set-up	42
Fig 4.5	Side view of experimental setup showing clamping arrangement	42
Fig 4.6	Photographic view of the spring loaded exciter with a dial gauge	43
Fig 4.7	Digital storage oscilloscope	43
Fig 4.8	Contact type vibration pick-up	44
Fig 4.9	Dial gauge mounted on a stand with magnetic base	45
Fig 4.10	Variation of μα with Natural frequency of vibration for mild steel specimens with beam thickness ratio 1.0 at different initial amplitudes of excitation (y) for non-uniform interface pressure	49
Fig 4.11	Variation of μα with Natural frequency of vibration for mild steel specimens with beam thickness ratio 1.5 at different initial amplitudes of excitation (y) for non-uniform interface pressure	49
Fig 4.12	Variation of μα with Natural frequency of vibration for mild steel specimens with beam thickness ratio 2.0 at different initial amplitudes of excitation (y) for non-uniform interface pressure	50
Fig 4.13	Variation of μα with Natural frequency of vibration for mild steel specimens with beam thickness ratio 1.0 at different initial amplitudes of excitation (y) for uniform interface pressure	50
Fig 4.14	Variation of μα with Natural frequency of vibration for mild steel specimens with beam thickness ratio 1.5 at different initial amplitudes of excitation (y) for uniform interface pressure	51
Fig 4.15	Variation of μα with Natural frequency of vibration for mild steel specimens with beam thickness ratio 2.0 at different initial amplitudes of excitation (y) for uniform interface pressure	51
Fig 5.1	Variation of logarithmic decrement with applied tightening torque of (2+2)×49.2 mm cross-section beam with length 393.6mm at different amplitude of excitation with thickness ratio 1.0 for non-uniform pressure at the interface.	53
Fig 5.2	Variation of logarithmic decrement with applied tightening torque of (2+3)×57.6 mm cross-section beam with length 460.8 mm at different	

amplitude of excitation with thickness ratio 1.5 for non-uniform pressure at the interface. 54
Fig 5.3 Variation of logarithmic decrement with applied tightening torque of (2+4)×66 mm cross-section beam with length 462 mm at different amplitude of excitation with thickness ratio 2.0 for non-uniform pressure at the interface. 54
Fig 5.4 Variation of logarithmic decrement with applied tightening torque of (3+3)×28.032 mm cross-section beam with length 364.416 mm at different amplitude of excitation with thickness ratio 1.0 for uniform pressure at the interface. 55
Fig 5.5 Variation of logarithmic decrement with applied tightening torque of (2+3)×28.812 mm cross-section beam with length 374.556 mm at different amplitude of excitation with thickness ratio 1.5 for uniform pressure at the interface 55
Fig 5.6 Variation of logarithmic decrement with applied tightening torque of (3+6)×28.92 mm cross-section beam with length 375.96 mm at different amplitude of excitation with thickness ratio 2.0 for uniform pressure at the interface 56
Fig 5.7 Variation of logarithmic decrement with initial amplitude of excitation for mild steel specimen of thickness ratio 1.0 for non-uniform interface pressure with beam length 344.4 mm and thickness (3+3)×49.2 mm having bolt diameter 12 mm at 2.5 lb ft tightening torque 56
Fig 5.8 Variation of logarithmic decrement with initial amplitude of excitation for mild steel specimen of thickness ratio 1.5 for non-uniform interface pressure with beam length 403.2 mm and thickness (3+4.5)×57.6 mm having bolt diameter 12 mm at 5 lb ft tightening torque 57
Fig 5.9 Variation of logarithmic decrement with initial amplitude of excitation for mild steel specimen of thickness ratio 2.0 for non-uniform interface pressure with beam length 528 mm and thickness (2+4)×66 mm having bolt diameter 12 mm at 10 lb ft tightening torque 57
Fig 5.10 Variation of logarithmic decrement with initial amplitude of excitation for mild steel specimen of thickness ratio 1.0 for uniform interface pressure with beam length 364.416 mm and thickness (2+2)×28.032 mm having bolt diameter 12 mm at 5 lb ft tightening torque 58
Fig 5.11 Variation of logarithmic decrement with initial amplitude of excitation for mild steel specimen of thickness ratio 1.5 for uniform interface pressure with beam length 374.556 mm and thickness (3+4.5)×28.812 mm having bolt diameter 12 mm at 5 lb ft tightening torque 58
Fig 5.12 Variation of logarithmic decrement with initial amplitude of excitation for mild steel specimen of thickness ratio 2.0 for uniform interface pressure with beam length 375.96 mm and thickness (2+4)×28.92 mm having bolt diameter 12 mm at 2.5 lb ft tightening torque 59
Fig 5.13 Variation of logarithmic decrement with length of mild steel specimens of cross-section (3+3)×49.2 mm at 0.3 amplitude of excitation with thickness ratio 1.0 for non-uniform interface pressure at 2.5 lb ft tightening torque. 59
Fig 5.14 Variation of logarithmic decrement with length of mild steel specimens of cross-section (3+4.5)×57.6 mm at 0.1 amplitude of

excitation with thickness ratio 1.5 for non-uniform interface pressure at 2.5 lb ft tightening torque 60

Fig 5.15 Variation of logarithmic decrement with length of mild steel specimens of cross-section (2+4)×66 mm at 0.5 amplitude of excitation with thickness ratio 2.0 for non-uniform interface pressure at 10 lb ft tightening torque 60

Fig 5.16 Variation of logarithmic decrement with length of mild steel specimens of cross-section (3+3)×28.032 mm at 0.1 amplitude of excitation with thickness ratio 1.0 for uniform interface pressure at 5 lb ft tightening torque 61

Fig 5.17 Variation of logarithmic decrement with length of mild steel specimens of cross-section (2+3)×28.812 mm at 0.1 amplitude of excitation with thickness ratio 1.5 for uniform interface pressure at 2.5 lb ft tightening torque 61

Fig 5.18 Variation of logarithmic decrement with length of mild steel specimens of cross-section (2+4)×28.92 mm at 0.1 amplitude of excitation with thickness ratio 2.0 for uniform interface pressure at 2.5 lb ft tightening torque 62

Fig 5.19 Variation of logarithmic decrement with number of layers for uniform interface pressure with thickness 2h=2 mm and length of beam is 364.416 mm of thickness ratio 1.0 62

Nomenclature

English Symbols

A	Area of cross-section of the beam
A_0	Area of cross-section of the bolt
A'	Area under the connecting bolt head
d	Diameter of the connecting bolt
E	Static bending modulus of elasticity
E_f	Energy loss per cycle due to friction at joints
E_{loss}	Total energy loss per cycle
E_n	Energy stored in the system per cycle
E_0	Energy loss per cycle due to material and support friction
F_{rM}	Maximum frictional force at the interfaces
$2h_1$, $2h_2$	Thickness of each layer of the cantilever specimen
I	Second moment of area
K	Static bending stiffness of the layered and jointed beam
k'	Static bending stiffness of the solid beam
l	Length of individual elements
L	Free length of the layered and jointed beam
m	Number of layers in a jointed beam
N	Total normal force under each connecting bolt
p	Interface pressure
P	Preload on a bolt
T	Tightening torque on bolt
q	Number of bolts
R	Any radius within influencing zone
R_B	Radius of the connecting rivet
R_M	Limiting radius of influencing zone
t	Time coordinate
u_0	Relative dynamic slip between the interfaces at a riveted joint in the absence of friction
u_r	Relative dynamic slip between the interfaces at a riveted joint in the

	presence of friction
u_{rM}	Relative dynamic slip between the interfaces at the maximum amplitude of vibration
W	Static load
a_1, a_{n+1}	Amplitude of first cycle and last cycle, respectively
$y(l, 0)$	Initial free end displacement
n	Number of cycles

Greek Symbols

α	Dynamic slip ratio(u_r/u_0)
δ	Logarithmic decrement of the system
δ_f	Logarithmic decrement due to interface friction
δ_0	Logarithmic decrement due to internal and support friction
Δ	Deflection due to static load
μ	Kinematic coefficient of friction
ω_n	Natural frequency of vibration
ω_d	Damped frequency of vibration
ρ	Mass density
σ_0	Initial stress on a bolt
σ_s	Surface stress on the jointed structure
ζ	Damping ratio
ψ	Specific Damping capacity

CHAPTER-1

INTRODUCTION

1.1 Background

In every machine structures vibration is an undesirable effect. To minimize this effect, research is going on throughout the globe by increasing the damping capacity of these structures. Due to uncontrolled vibration, internal stresses are generated in the structures, which result in their premature failure. With the rapid growth and development of the engineering structures, various works have been reported on the improvement of damping capacity of these structures for controlling the disastrous effects of vibrations. In order to reduce the vibration effects and enhance the damping characteristics, machines are made lighter and fabricated in layers instead of monolithic structures. Structures are assembled by various techniques and fabricated as jointed, welded, sandwich structures etc. The jointed structures are manufactured with the help of fasteners such as bolts and rivets etc.

The study of structural dynamics is very essential to predict the damping under different vibration conditions. In almost all machines vibration is kept as low as possible. Whenever a structural member is excited with some frequency, and in the event of natural frequency of the external force coinciding with any one of the natural frequencies of the structure, a situation called “resonance” occurs. This resonance creates an undesirable vibration causing failure in most of the structural members. Presently low weight structures are used in many structural applications. In order to improve the damping capacity of structures, special design techniques such as structural members of visco-elastic layers, multi-layered sandwich, high elastic inserts in the parent material, layered structures jointed with bolts, welds and rivets etc. are normally used in actual practice.

When two layers of a structure are joined together, relative slip occurs at the interface which results in friction. Due to this friction energy is dissipated thereby increasing the damping capacity of the system. In built-up structures, joints play significant role in arising this friction due to interface slip between the layers. Beards [34] has established that 90% of damping in fabricated structure is due to joints only. By

proper designing, system damping characteristics can be improved significantly in jointed structures.

The energy dissipation in jointed structures is influenced by many vital parameters such as; interface pressure, tightening torque, coefficient of friction, relative dynamic slip, length and thickness ratio of beam layers, amplitude and frequency of vibration etc.

1.2 Motivation

Almost all built-up structures are fastened with the help of bolts, rivets and welds. Due to these fasteners interface pressure exists between the two layers of beam. This interface pressure is maximum at the surface of the joint and gradually decreases towards the far end of the influence zone. The shape of the interface pressure profile is parabolic in nature thus depicting the non-uniform nature of interface pressure. Many works related to the bolted and riveted joints with non-uniform interface pressure has been reported till date but a little amount of work has been done on the bolted structure with uniform intensity of pressure at the interfaces. Improvement in damping capacity of built-up structures fabricated with welded and riveted joints is not so much pronounced as compared to the structures fabricated with bolted joints [1].

For the improvement of damping capacity of the structures the bolted joint is found to be the proper option, then the riveted and welded joints. As we know from the earlier studies that though the fundamentals of damping mechanism is same in both bolted and riveted joints, they differ from each other in different aspects. In case of bolted joints the preloaded pressure can be varied by varying the tightening torque but in case of riveted joint it is a fixed quantity. The interface pressure and spacing between the two consecutive fasteners are different in both the cases. Hence, the damping capacity for both the structures is different.

The present work focuses in developing the theory of damping mechanism in bolted multi-layered beam structures using classical energy approach with both non-uniform and uniform pressure at the interface considering different thickness ratio.

1.3 Beam theories

In a dynamic structure beam is one of the elementary object. In various structural member beams play a vital role in the construction of various parts such as in bridges, body of robots, aerospace rotor blades and other aerospace components, towers, machine structures, etc. These beam structures are classified by their cross-section area, length and materials used etc. According to their cross-section it is classified in to thick and thin beam. To study the dynamic characteristics of the beam element two types of theories are adopted;

(i) Euler-Bernoulli beam theory.

(ii) Timoshenko beam theory,

Various dynamic behaviour of the beam structure can be analyzed using the above two theories. Thin and thick beams are analyzed with the help of Euler-Bernoulli beam theory and Timoshenko beam theory respectively. In the present work the theory of thin beam, i. e., the Euler-Bernoulli beam theory is used as the width of the beam is less than one tenth of its length. Moreover, the beam is excited to vibrate at low natural frequency.

1.4 Outlines of the thesis

The research presented in this thesis gives a framework on the study of the damping capacity and its enhancement in bolted jointed structures due to energy dissipation by joint friction and dynamic micro-slip at the interface. The investigation as outlined in this thesis is broadly divided into seven chapters. The thesis work is outlined as follows;

Chapter 1: This chapter gives a brief introduction to the thesis work and summarizes the importance, motivation of the present investigation.

Chapter 2: This chapter contains a detailed relevant literature review on various aspects of vibration analysis of layered and jointed structures. Most of the earlier and present vital researches carried out by various scientists have been represented in details. This chapter is divided into different sections emphasizing; types of damping, mechanisms of damping, various vibration terminologies and techniques used for improving the damping.

Chapter 3: This chapter elaborates a complete description of the theoretical analysis by classical energy approach considering dynamic slip ratio for determining the damping capacity in bolted cantilever beams. The theoretical expression for the uniform pressure distribution has been found out by considering the different layers in perfect contact. This interface pressure distribution has been further applied to estimate the logarithmic damping decrement for layered beams with unequal thickness ratios as well as for multi-layered bolted beams.

Chapter 4: This chapter outlines the details of the experimental set-up, instrumentation, sample preparation and different testing methods for the measurement of damping. In actual practice, the experimental measurement of logarithmic damping decrement becomes necessary because of the fact that the theoretically computed damping capacity of a structure may be different from that of the actual values due to assumptions made in the theoretical analysis. Damping of these structures has been experimentally measured in terms of logarithmic decrement using the time signals with the help of storage oscilloscope. Experimental results for different set of layered and bolted mild steel specimens have been compared with the corresponding numerical values obtained in chapter-3 for establishing the authenticity of the theory developed. These comparative results are presented in graphical and tabular forms in the successive chapters.

Chapter 5: This chapter elaborates the detailed discussions on the results obtained from the theoretical and experimental analysis as outlined in chapters 3-4.

Chapter 6: This chapter summarizes the important conclusions drawn from the observations discussed in the chapter 5 along with some suggestions for applying the present work in various fields of real applications. This chapter also contains the scope for further research work.

CHAPTER-2

LITRETURE REVIEW

2.1 Introduction

All most all the dynamic structures are subjected to obscure vibrating conditions. This vibration may create many undesirable effects on the structural element. To reduce the effect of vibration and enhance the damping property of the dynamic structures various techniques such as; jointed structures with fasteners like bolt, rivet and weld, inclusion of visco-elastic layers and multi-layered sandwich structure, elastic inserts are applied. A lot of work has been done on bolted jointed structures with non-uniform interface pressure between the two layers of the beam but a few amount of work has been reported on uniform pressure at the interface of the beam. The damping of the structures with uniform intensity of interface pressure has been reported to be more compared to that of the non-uniform pressure distribution. The present chapter elaborates the detailed literature surveys on earlier and present research works on bolted cantilever beams.

2.2 Vibration and damping

Most of the engineering structures possess inherently low damping properties causing the unpredicted failure of the structural members. The vibration creates many undesirable effects in the dynamic system which is minimized due to presence of damping. It reduces the amplitude of vibration by dissipating the vibration energy in the form of friction between the two layers of system. For the proper design and operation of a dynamic system the exhaustive study of the damping is very essential. In some cases damping is intentionally reduced, such as tuning fork, musical instruments, loudspeaker, vibratory conveyers, and compactors. But in most of the machine structures damping is increased to reduce the chances of fatigue failure.

The damping is further divided into three types, such as,

(i) Material damping
(ii) Structural damping
(iii) Fluid damping

2.2.1 Material damping

Material damping is also known as internal damping. Energy dissipation in material damping occurs at molecular level. Micro structure defects are the main cause of energy dissipation. The thermo elastic effect, eddy current effect and dislocation motion in metals occur in material damping. The magnitude of material damping in structural members is less. So, some structural materials, like iron, steel, or aluminum are having less damping capacity than Ferro-magnetic materials and alloys of magnesium and cobalt.

2.2.2 Structural damping

Structural damping occurs at the joints present in the structure. Structural damping is the result of the mechanical-energy dissipation caused by rubbing friction initiating from relative motion between components of the structural members. Structural damping is also classified into three types, such as,

(1) Support damping

(2) Damping due to sandwich construction

(3) Damping due to joints

2.2.3 Fluid damping

Fluid damping may arise from the structure and the fluid surrounding it. Structural damping is related to the properties of the structure itself, where the fluid damping is due to viscous dissipation and fluid drag, i.e., it is the result of viscous shearing of the fluid at the surface of the structure and of flow separation.

2.3 Measurement of structural damping

Energy dissipation in structural damping caused due to the rubbing or impacting can be represented by Coulomb-friction model. There are two types of vibration such as natural vibration and forced vibration. In natural vibration the system is allowed to vibrate at one or more natural frequency and then gradually damped down to zero amplitude. In forced vibration an additional force or motion is applied to a mechanical system.

There are two methods used in measurement of the damping of a structure. Such as, time response and frequency response. In time response, the response of the system is represented as time domain and in frequency response, the system is expressed as frequency domain respectively. The use of the above two methods depends on the

mathematical model of the system. Using the time domain method logarithmic decrement δ is determined and in frequency domain method the quality factor Q is determined. Whereas, the other nomenclatures such as; damping ratio ζ, loss factor η and specific damping capacity ψ are estimated from either of the above two methods for measuring the damping [7].

2.3.1 Logarithmic decrement (δ)

Logarithmic damping decrement plays a vital role to find-out the damping capacity of a dynamically loaded structure. It is generally used in time response method. The different factors that influence the logarithmic damping decrement are dynamic slip and interface pressure at the contacting surfaces. The logarithmic damping decrement, δ, is usually expressed as,

$$\delta = \frac{1}{n} \ln \left(\frac{a_1}{a_{n+1}} \right)$$

where, a_1 is amplitude of vibration at certain time and a_{n+1} is the amplitude of vibration after elapse of n cycles.

2.3.2 Damping ratio

The damping can also be measured by measuring the damping ratio which gradually reduces oscillation with time in a harmonic system. When a cantilever beam is vibrated with a natural frequency; its amplitude of vibration reduces to zero after some time. Due to the friction at the joints the energy loss occurs in the system. It is observed that the amplitude of vibration decays more rapidly as the value of the damping ratio increases as shown in Fig 2.1 below.

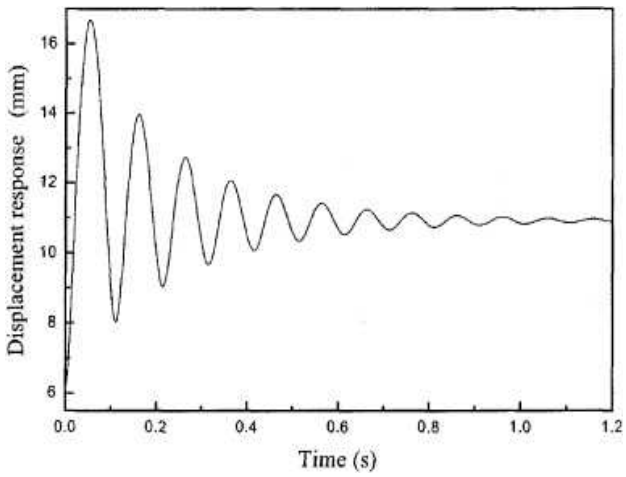

Fig.2.1 Free vibration damping system

To characterize the amount of damping in a system, a ratio called the damping ratio (also known as damping factor) is used. This damping ratio is just a ratio of the actual damping over the amount of damping required to reach critical damping. The formula for the damping ratio (ζ) of the mass spring damper model is:

$$\zeta = \frac{c}{2\sqrt{km}}$$

where, *c*, *k* and *m* are the damping constant, system stiffness and mass, respectively.

The damping ratio is dimensionless, being the ratio between two coefficients of identical units.

2.3.3 Specific damping capacity (ψ)

Specific damping capacity, ψ, is the ratio between energy dissipated due to the relative dynamic slip at the interfaces and the total energy introduced into the system and is found to be;

$$\psi = \left[E_{loss} / \left(E_{loss} + E_{ne} \right) \right] = 1 / \left[1 + E_{ne} / E_{loss} \right]$$

where, E_{loss} and E_{ne} are the total energy loss due to interface friction and the total energy introduced in to the system, respectively.

2.4 Improvement of damping capacity of structures

The structural members inherently possess low damping characteristic. For the enhancement of the damping ratio in a system various measures has been adopted by the technologists. To increase the damping capacity some external energy dissipating sources are incorporated in to the dynamic system. Some of the techniques used are,

(i) Use of unconstrained and constrained visco-elastic layers
(ii) Use of special high damping inserts
(iii) Use of layered and jointed constructions

2.4.1 Use of unconstrained and constrained visco-elastic layers

2.4.1.1 Unconstrained layer or external damping

A visco-elastic material possesses both viscous and elastic characteristic. Some of the energy stored in a visco-elastic system is recovered upon the removal of the load and

the remainder is dissipated in the form of heat. Visco-elastic damping is also known as passive damping.

The unconstrained damping is also called as extensional damping of a structure. In this technique the damping material is applied over the entire surface of the structure. It is one of the simplest forms of visco-elastic material applications as shown in Fig 2.2.

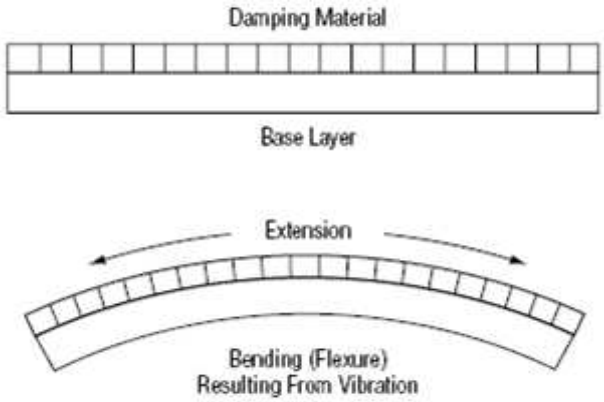

Fig.2.2 An un-constrained-layer damping system

In this the viscoelastic layer is applied to the whole surface of the structure with the help of a bonding material. When the layer is subjected to alternate extension and compression, then the elastic layer to which it is bonded experiences flexural vibrations. It is widely applied to finished material structures like automobile bodies, ship hulls, and aerospace industry.

2.4.1.2 Constrained-layer Damping

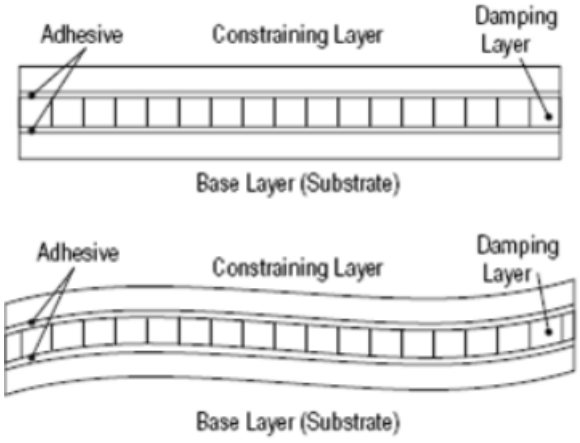

Fig.2.3 A constrained-layer damping system

In constrained-layer damping the visco-elastic layer is sandwiched between two layers of the structure with a thin layer of high damping material. When the base structure is

subjected to a dynamic load, the damping layer also tends to be loaded with shear strain thereby dissipating energy. The constrained layer damping is used in aerospace, missile structure, building, bridges and ship engines. Cyclic damping produced in thin layers of dissipative material placed between two rigid surfaces is increased with the decrease of adhesive layer thickness.

2.4.2 Use of special high damping inserts

The damping capacity of a dynamically loaded structural member is increased by inserting special high damping inserts. These special inserts can be attached with the help of welding or press fit process. It has been observed that the damping capacity of aluminium cantilever strips can be increased by using high damping inserts of different materials, such as, Cast Iron, Bakelite and Perspex. It has been found that the damping capacity of welded inserts is less than that of damping characteristics of press fit inserts.

2.4.3 Use of layered and jointed constructions

Layered and jointed mechanical structure is one of the most useful structure in which damping is high due to the presence of joints in the member. It has been established that the welded structure possesses less damping compared to that of the bolted or riveted jointed structure. The total damping is much more than the sum of the material damping of individual elements of the structure. The damping in a beam like structure is increased by fabricating a metal in layered bolted structure rather than solid structure. In layered structure interfacial slip occurs between the layers of the structure. There energy loss occurs at the interfaces only due to interfacial slip and friction between the layers. This type of jointed structures is widely used in the construction of bridges, frames, gas turbines and aerospace parts etc. The present research work is mainly focused on layered and jointed structures so as to increase the damping capacity of the system. A detailed literature study on the layered and interfacial jointed damping is presented in the succeeding section.

2.5 Review of literature on jointed structures

With the rapid change in structural engineering material design, the enhancement of damping has become the most challenging subject for the present researchers. Most of the monolithic structures possess poor damping making it unsuitable for engineering applications. A lot of research is going on around the globe to improve the damping

capacity of structures using different techniques. A number of techniques used for the enhancement of damping in structural members are inserting visco-elastic layers, multi-layered sandwich, high elastic inserts in the parent material, layered structures jointed with bolts, welds and rivets etc. Damping in built-up structures mainly occurs from two types of sources such as, internal damping or material damping which is very low as compared to the other one structural damping [9,18]. Structural damping is the damping which is produced due to the joints present in the system. It is established that the bolted and riveted joints are the fasteners which contribute about 90% of the damping to the built-up structures [3, 5, 35, 42]. Damping properties of bolted structures can be enhanced by changing the thickness ratio of the beams and also by changing the diameter of the bolts. The damping capacity can also be enhanced by manufacturing the product in layered structure. However, the attention has to be focused on the orientation and spacing of the connecting bolts to increase the damping capacity. It is established that the joints usually exhibit two types of motions; micro-slip and macro-slip [15, 21, 30]. With the application of low external force, slip occurs at the interfaces. This type of slip is called as micro-slip. Most of the dynamic structures are excited with low amplitude of excitation. If the structures are applied with high amplitude of excitation, then the type of slip occurs is called macro-slip which may damage the structural member without dissipating energy and reducing the life of the structure. A lot of research has been done by various engineers till now related to micro-slip in jointed structures and enhancement of damping capacity by the theory of micro-slip [18]. Many researchers [23, 29] have utilized the micro-slip concept considering the friction surface as an elastic body. As established [2] the bolted and other mechanical joints are the major source of energy dissipation which increases the damping in the jointed structures.

Earlier researchers [29, 34, 39] have carried out extensive work on the bolted joints assuming uniform intensity of pressure distribution at the interfaces of the layered structures without considering the effects of surface irregularities and asperities. A lot of work has been done on the pattern and intensity of pressure distribution at the interfaces of bolted joints and the damping characteristics of jointed structures [6, 13, 14, 20, 26, 27, 44, 46, 48].

Although lot of research has been done on damping capacity of bolted beams with equal thickness ratio and non-uniform pressure at the interface, few amount of work

has been reported relating to bolted beam with unequal thickness ratio and uniform pressure at the interface. The present work in this thesis is based on the investigation of damping capacity of the beam structures with bolted joints having unequal thickness ratio and uniform pressure at the interface. Also the energy dissipation in this system occurs due to the micro-slip and friction present at the interface.

Some researchers [12, 40] have established that the micro-slip at the contacting surfaces occur when an optimal frictional load is applied on the structure. They have also investigated a model for micro-slip between the flat smooth and rough surfaces covered with ellipsoidal elastic bodies. This shows that the role of micro-slip and friction are of supreme importance in controlling the dynamic characteristics of engineering structures. The friction may be undesirable or desirable depending on the type of applications. Friction is often considered damaging in nature in the design of moving parts. On the other hand, this is desirable in fabricated structures for effective energy dissipation. The friction at the bolted layers originates when the consecutive layers experience relative movement under low amplitude loading of transverse vibration. The Coulomb's law of friction is widely used to represent the dry friction at the contacting surfaces. The friction in a joint arises from shearing between the parts and is governed by the torque on the bolt, surface properties and type of materials in contact [16].

The steady state response of a simple friction-damped system with combined Coulomb and viscous friction problem has been analytically solved by Den Hartog [12]. Many engineers have presented in their review that micro-slip and friction in structural joints is regarded as the main source of energy dissipation and enhances the damping capacity of the system [13, 17, 45].

As discussed earlier, structural damping offers a large amount of energy dissipation due to the presence of micro-slip and interface shear of the joint. It is thus established that the jointed and layered structure contributes highest damping capacity to all fabricated structures.

Various factors that affect the damping capacity of the structures are interface pressure, diameter of bolt, length and thickness ratio of the beam, etc. The nature of pressure distribution across a beam layer is an important feature affecting the damping capacity of jointed structures. Many engineers have tried over the years to find-out the actual pattern of pressure distribution at the interfaces due to the clamping action by the fasteners. Earlier, some researchers have idealized the joints by assuming a

uniform pressure profile without considering the effects of surface irregularities and asperities [38, 40, 47]. Later on many authors [19, 26, 44, 48, 50] have conducted experiments to ascertain the exact pressure distribution characteristics. These experiments have confirmed that the interface pressure is not uniform in actual pattern.

Gould and Mikic [19] and Ziada and Abd [50], have shown that the pressure distribution at the interfaces of a bolted joint is not uniform but parabolic in nature. This interface pressure exists on an influence zone in the form of a circle with 3.5 times the diameter of the connecting bolt which is independent of the tightening load applied on it as shown in Fig 3.3.

Further work has been reported by Nanda and Behera [36] on the distribution pattern of the interface pressure where they have evaluated the damping capacity of layered and jointed structures in bolted joints. They developed a theoretical solution for the pressure distribution at the interfaces of a bolted joint by curve fitting the earlier data reported by Ziada and Abd [50]. They obtained an eighth order polynomial even function in terms of normalized radial distance from the centre of the bolt such that the function assumes its maximum value at the centre of the bolt and gradually decreases away from the bolt diameter surface. Dunn's curve fitting software was used by them to calculate the exact spacing between the consecutive bolts that would result in a uniform interfacial pressure distribution along the entire length of the beam. Using exact spacing of 2.00211 times the diameter of the connecting bolts, Nanda and Behera [36] have investigated the damping capacity of a beam structure having uniform interface pressure over the length of the beam.

Later, Nanda [37] has shown the distribution pattern of the interface pressure and evaluated the damping capacity of layered and jointed structures in bolted joints and established that the number of layers, diameter of the bolts and the relative spacing between the connecting bolts play major roles on the damping capacity of these structures. Researchers [4, 25, 49] has investigated the influence of joint tightness; joint spacing and surface finish on the energy dissipation and found that the energy dissipation rate depends on the magnitude of normal force between the connecting members.

Recently Damisa et al. [11] have carried out an investigation to study the effect of non-uniform pressure distribution on the mechanism of slip damping in layered beams, but their analysis is limited to static load. Later, they have extended their

analysis to realistic dynamic loading for estimating the interfacial slip damping in clamped layered beams [32]. They have shown that under dynamic loading, the factors like non-uniform pressure distribution as well as frequency variation affects significantly on both the energy dissipation and logarithmic decrement which are associated with the mechanism of slip damping in layered structures. They have further reported that the amount of energy dissipation through slip damping under externally applied dynamic load is less than that of the corresponding static load. Olunloyo et al. [10] have used other forms of pressure distributions such as polynomial or hyperbolic representations but the results obtained have demonstrated that the effects of such distributions in comparison with the linear profile are largely incremental in nature.

There are various methods available to estimate the contact pressure between two layers of the structure. The measurement of almost real contact pressure without changing the characteristics of the contact surface by using ultrasonic waves has produced fair results using a normal probe is found to be the best technique [22, 31].

Earlier, some researchers have established the relation between the amplitude of excitation and damping capacity; with increase in amplitude of excitation the logarithmic decrement also increases [24].

Minakuchi et al. [31] have also used angle probe to find out the contact pressure between two layered beams of different thicknesses by establishing a relationship between the mean contact pressure and sound pressure of reflected waves. This method is widely accepted, as the experimental results fairly agree with the theoretical ones. The present investigation uses the numerical data of Minakuchi et al. [31] to obtain the theoretical equation for non-uniform and uniform pressure at the interfaces of a jointed beam by using MATLAB software for fitting the pressure curves.

All the previous research deals with the beams of equal thickness ratio whereas the objective of the present work is to evaluate theoretically the damping capacity of the bolted cantilever beam with unequal thickness ratio under non-uniform and uniform intensity of pressure distribution at the interfaces and compare it with experimental results for validating the theory developed by using energy approach.

CHAPTER-3

THEORETICAL ANALYSIS BY CLASSICAL ENERGY APPROACH

3.1 Introduction

It is established from the previous chapters that the joints are the major source of energy dissipation in built-up structures. The damping in jointed structure is due to the frictional energy loss occurring at the interfaces of the layers. The damping capacity of the jointed structure can be enhanced by manufacturing layered structure, varying the length of the specimen and tightening torque etc. The damping capacity is also governed by the factors, such as; intensity of pressure distribution, micro-slip and kinematic coefficient of friction at the interfaces etc. For accurate evaluation of energy loss and the damping capacity in jointed structures, all these parameters are to be considered.

The current chapter presents a thorough description of the theoretical analysis by classical energy approach for determining the damping capacity in layered and bolted cantilever beams with unequal thickness ratio. The interface pressure curve between the two layers of beam is taken from Minakuchi [31] and evaluated using MATLAB software. Both non-uniform and uniform pressure is considered for the evaluation of the damping property.

There are two types of beam models used in the vibration problems. They are Euler-Bernoulli and Timoshenko models. The Timoshenko beam model takes into account shear deformation and rotational inertia effects, making it suitable for describing the behaviour of short beams, sandwich composite beams or beams subjected to high frequency of excitation. Euler-Bernoulli beam model is known as classical beam model. This model is used for calculating small deflections of beam. In the present work Euler-Bernoulli beam theory is used for the evaluation of the damping capacity of beam.

The general assumptions taken for the analysis of the cantilever beam are;

- Each layer of the beam undergoes the same transverse deflection.
- The initial excitation at the free end of the beam is of small amplitude.
- There is no macro-slip in the joint.

- The local mass of the joint area is not considered as significant in altering the behavior of the beam.
- The circular holes for inserting bolts on the test specimens are completely filled by the bolts.
- There is no displacement and rotation of the beam at the clamped end.
- The Coulomb law of friction is used.
- The material behaves linearly.
- The deflections are small compared to the beam thickness.
- The effects of rotary inertia and shear deformation are neglected.

3.2 Dynamic equations of free transverse vibration of cantilever beam

When a cantilever beam is subjected to some load at its free end, it undergoes free vibration with transverse displacement *y(x, t)*. This transverse displaced beam is shown in Fig 3.1. In formulating the dynamic equations, Euler-Bernoulli beam theory is used on the assumptions that the rotation of the differential element is negligible compared to translation and the angular distortion due to shear is small in relation to bending deformation. This assumption is valid in the case when the ratio of the length of the beam to its depth is large. The present work is related to this type of investigation where a long beam is used.

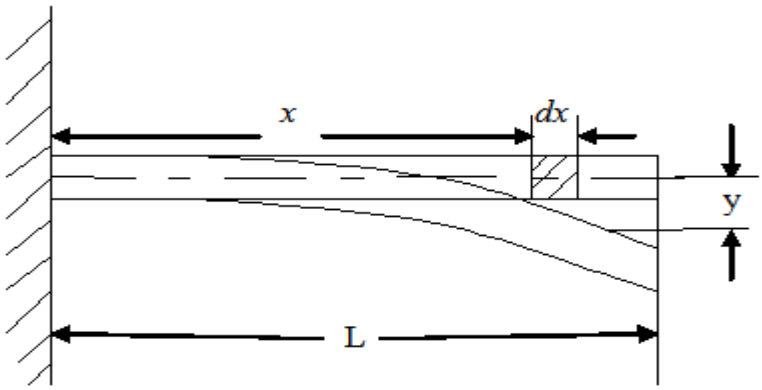

Fig.3.1 Free transverse vibration of a beam

The beam vibration is governed by the partial differential equations in terms of two variables for space function *x* and time function *t*. Therefore, the governing differential equation for the free transverse vibration of a beam is represented by;

$$E\ I\ \frac{\partial^4 y(x,t)}{\partial x^4} + \rho\ A\ \frac{\partial^2 y(x,t)}{\partial t^2} = 0 \tag{3.1}$$

where E, I, ρ and A are modulus of elasticity, second moment of area, mass density and cross-sectional area of the beam, respectively.

The free vibration given in Eq. (3.1) contains four spatial derivatives and therefore requires four boundary conditions for getting a solution. The presence of two time derivatives again requires two initial conditions, one for displacement and another for velocity.

The above Eq. (3.1) is solved by method of *separation of variables.* The displacement $y(x,t)$ is written as the product of two functions, i. e., one depends only on space function x and other depends only on time function t. Thus the solution is expressed as:

$$y(x,t) = X(x) \times T(t) \tag{3.2}$$

where, *X(x)* and *T(t)* are the space function and time function respectively.

Putting Eq. (3.2) in Eq. (3.1), we get;

$$E\ I\ T(t)\ \frac{\partial^4 X}{\partial x^4} = -\rho\ A\ X(x)\ \frac{\partial^2 T}{\partial t^2} \tag{3.3}$$

Dividing Eq. (3.3) by *X (x)*T (t)* on both sides, variables are separated as;

$$\frac{\left(\frac{d^2 T}{dt^2}\right)}{T(t)} = -\frac{E\ I}{\rho\ A}\frac{\frac{d^4 X}{dx^4}}{X(x)} = \omega_n^2 \tag{3.4}$$

where the term ω_n^2 is the separation constant, representing the square of natural frequency.

This equation gives two ordinary differential equations.

The first one is given as;

$$\left(\frac{d^4 X}{dx^4}\right) - \lambda^4 X(x) = 0 \tag{3.5}$$

where

$$\lambda^4 = \frac{\rho\ A}{E\ I}\omega_n^2 \tag{3.5a}$$

The required solution of Eq. (3.5) is simplified as;

$$X(x) = A_1 \sin \lambda x + A_2 \cos \lambda x + A_3 \sinh \lambda x + A_4 \cosh \lambda x \tag{3.6}$$

where the constant A_1, A_2, A_3 and A_4 are determined from the boundary conditions of cantilever beam.

The second equation is given as;

$$\left(\frac{d^2 T}{dt^2} \right) + \omega_n^2 T(t) = 0 \tag{3.7}$$

This is the free vibration expression for an un-damped single degree of freedom system having the solution

$$T(t) = A_5 \cos \omega_n t + A_6 \sin \omega_n t \tag{3.8}$$

Substituting the expression for space and time function as given by Eq. (3.6) and Eq. (3.8) into Eq. (3.2), the complete solution for the deflection of a beam at any section is expressed as;

$$y(x,t) = (A_1 \sin \lambda x + A_2 \cos \lambda x + A_3 \sinh \lambda x + A_4 \cosh \lambda x) \times (A_5 \cos \omega_n t + A_6 \sin \omega_n t) \tag{3.9}$$

3.2.1 Evaluation of Constants A_1, A_2, A_3 and A_4

The boundary conditions for the cantilever beam of the above Eq. (3.9) are given by;

At the fixed end: $x = 0, X(0) = 0, \frac{dX(0)}{dx} = 0;$

At the free end: $x = l, \frac{d^2 X(l)}{dx^2} = 0$

Writing the expression of space function as given in Eq. (3.6), its first derivatives are written as;

$$X(x) = (A_1 \sin \lambda x + A_2 \cos \lambda x + A_3 \sinh \lambda x + A_4 \cosh \lambda x) \tag{3.10}$$

$$X'(x) = \lambda (A_1 \cos \lambda x - A_2 \sin \lambda x + A_3 \cosh \lambda x + A_4 \sinh \lambda x) \tag{3.11}$$

Putting the above boundary conditions, Eq. (3.10) is reduced to;

$$X(0) = A_2 + A_4 = 0 \tag{3.12a}$$

$$\frac{dX(0)}{dx} = A_1 + A_3 = 0 \tag{3.12b}$$

$$X(l) = (A_1 \sin \lambda l + A_2 \cos \lambda l + A_3 \sinh \lambda l + A_4 \cosh \lambda l)$$

$$\frac{d^2X(l)}{dx^2} = \lambda^2(-A_1 \sin \lambda l - A_2 \cos \lambda l + A_3 \sinh \lambda l + A_4 \cosh \lambda l) = 0$$
$$\Rightarrow \frac{d^2X(l)}{dx^2} = -A_1 \sin \lambda l - A_2 \cos \lambda l + A_3 \sinh \lambda l + A_4 \cosh \lambda l = 0 \quad (3.12c)$$

$$\frac{d^3X(l)}{dx^3} = \lambda^3(-A_1 \cos \lambda l + A_2 \sin \lambda l + A_3 \cosh \lambda l + A_4 \sinh \lambda l) = 0$$
$$\Rightarrow \frac{d^3X(l)}{dx^3} = (-A_1 \cos \lambda l + A_2 \sin \lambda l + A_3 \cosh \lambda l + A_4 \sinh \lambda l) = 0 \quad (3.12d)$$

Eq. (3.12) can be rewritten in a compact matrix form as;

$$\begin{bmatrix} 0 & 1 & 0 & 1 \\ 1 & 0 & 1 & 0 \\ -\sin \lambda l & -\cos \lambda l & \sinh \lambda l & \cosh \lambda l \\ -\cos \lambda l & \sin \lambda l & \cosh \lambda l & \sinh \lambda l \end{bmatrix} \begin{pmatrix} A_1 \\ A_2 \\ A_3 \\ A_4 \end{pmatrix} = \begin{pmatrix} 0 \\ 0 \\ 0 \\ 0 \end{pmatrix} \quad (3.13)$$

This vector equation can have a nonzero solution for the vector $[A_1\ A_2\ A_3\ A_4]^T$ only if the determinant of the coefficient matrix becomes equal to zero, the characteristic equation is given as;

$$\begin{bmatrix} 0 & 1 & 0 & 1 \\ 1 & 0 & 1 & 0 \\ -\sin \lambda l & -\cos \lambda l & \sinh \lambda l & \cosh \lambda l \\ -\cos \lambda l & \sin \lambda l & \cosh \lambda l & \sinh \lambda l \end{bmatrix} = 0$$

$$\Rightarrow \cos \lambda l . \cosh \lambda l = -1 \quad (3.14)$$

This transcendental equation is the required condition for the co-efficient matrix to give a non-trivial solution and can be further used to determine the frequencies of vibration. The Eq. (3.13) can be expressed into four algebraic equations. The constants A_2, A_3, and A_4 are dependent parameters and A_1 is an independent parameter. A_1 may have any value. Taking A_1=1, the values of constants of A_2, A_3 and A_4 are found as;

$$A_2 = \left(\frac{\sin \lambda l + \sinh \lambda l}{\cos \lambda l + \cosh \lambda l}\right), A_3 = -1, A_4 = -\left(\frac{\sin \lambda l + \sinh \lambda l}{\cos \lambda l + \cosh \lambda l}\right) \text{ and } A_1 = 1$$

Now space function given by Eq. (3.6) is modified as;

$$X(x) = (\sin \lambda x + \left(\frac{\sin \lambda l + \sinh \lambda l}{\cos \lambda l + \cosh \lambda l} \right) \cos \lambda x - \sinh \lambda x - \left(\frac{\sin \lambda l + \sinh \lambda l}{\cos \lambda l + \cosh \lambda l} \right) \cosh \lambda x)$$

$$X(x) = \frac{(\sin \lambda x - \sinh \lambda x)(\cos \lambda l + \cosh \lambda l) + (\cos \lambda x - \cosh \lambda x)\left(\sin \lambda l + \sinh \lambda l \right)}{\cos \lambda l + \cosh \lambda l}$$

This equation gives the different mode shapes of vibration.

The free vibration given by Eq. (3.1) contains four spatial derivatives and hence requires four boundary conditions for getting a solution. The presence of two time derivatives again requires two initial conditions, one for the displacement and another for velocity.

3.2.2. Evaluation of constants A_5 and A_6

The general expression of deflection at any section of the beam as given in Eq. (3.9) is written as;

$$y(x,t) = X(x) \times \left(A_5 \cos \omega_n t + A_6 \sin \omega_n t \right) \tag{3.15}$$

Taking the derivative with respect to time, the above equation reduces to;

$$y'(x,t) = X(x) \times \left(-A_5 \omega_n \sin \omega_n t + A_6 \omega_n \cos \omega_n t \right) \tag{3.16}$$

The velocity of deflection at the free end of the beam is zero.

i.e., $y'(l,0) = 0$ which yields A_6=0

Hence Eq. (3.15) reduces to;

$$y(x,t) = X(x) \times \left(A_5 \cos \omega_n t \right) \tag{3.17}$$

The deflection at the end of the beam is taken equal to *X(l)* and substituting the same in Eq. (3.17), we obtain;

$$y(l,0) = X(l) \times A_5$$

$$A_5 = \frac{y(l,0)}{X(l)};$$

Substituting the value of A_5 in Eq. (3.17), the final equation for the deflection is found to be;

$$y(x,t) = X(x) \times \left[\frac{y(l,0)}{X(l)} \right] (\cos \omega_n t); \tag{3.18}$$

i.e.,

$$y(x) = \begin{bmatrix} (\sin \lambda x - \sinh \lambda x)(\cos \lambda l + \cosh \lambda l) + \\ (\cos \lambda x - \cosh \lambda x)(\sin \lambda l + \sinh \lambda l) \end{bmatrix} \left[\frac{y(l,0)}{X(l)} \right] \frac{\cos \omega_n t}{\cos \lambda l + \cosh \lambda l}$$

3.3 Mechanism of micro slip

As stated earlier in the literature review, the maximum energy dissipation caused in a jointed structure is due to the micro slip at the interfaces between the two layers. Therefore, the study should be focused on mechanism of micro slip for the correct assessment of the energy dissipation for accurate damping assessment.

When the structural members are joined together with the help of fasteners and allowed for a small relative motion due to the application of a small transverse load, the slip takes place at the interfaces and is referred to as *micro slip*. This micro slip occurs over a small area of contact. The micro slip depends mainly on tightening force applied by the bolts. When the bolt is rigidly tightened, the structure behaves like a monolithic one. Moreover, when the fastener is kept less tight, the slip occurs over the entire surface of the structure and it is known as *macro slip*. The presence of this type of slip may cause the damage of the structure at the earlier stage. That is the reason for not considering it in the present work.

As investigated by the researchers the interface pressure is not uniform in nature. It is maximum at the surface of the bolt hole and decreases parabolically with the distance away from the bolt.

3.3.1 Determination of relative dynamic slip

Relative dynamic slip is evaluated assuming that the bending stiffness and bending conditions are same for each beam of the bolted cantilever beam while vibrating. Moreover, each layer of the beam shows no extension of the neutral axis and no deformation of the cross-section. When the jointed cantilever beam is given an initial excitation at the free end, then the contacting surfaces undergo relative motion called micro-slip. This relative displacement *u(x, t)* at any distance *x* from the fixed end in

the absence of friction is equal to the sum of Δu_1 and Δu_2 as shown in Fig. 3.2 and at a particular position and time is given by Masuko et al. [29] as;

$$u(x,t) = \Delta u_1 + \Delta u_2 = (h_1 + h_2)\tan[dy(x,t)/dx] \tag{3.19}$$

Whereas the actual dynamic slip $u_r(x,t)$ is less than the relative dynamic slip $u(x,t)$ due to the frictional energy loss and is given as,

$$u_r(x,t) = \alpha u(x,t) \tag{3.20}$$

where α is the dynamic slip ratio.

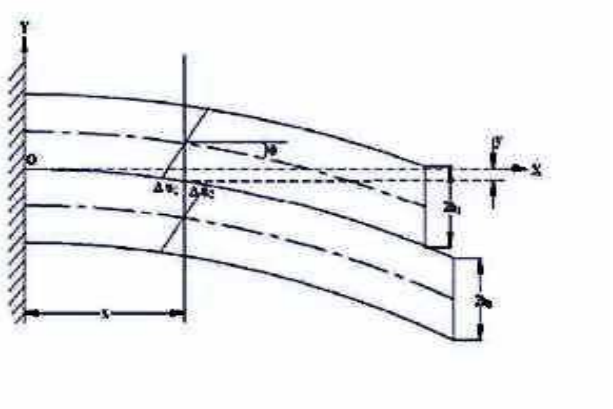

Fig. 3.2 Mechanism of dynamic slip at the interfaces

The maximum relative dynamic slip for non-uniform pressure under bolt has been reported by Mohanty and Nanda [33] and is given by;

$$u_{rM}(x,t) = 1/2\{\alpha(h_1 + h_2)X_{sum}\lambda y(l,0)\} \tag{3.21}$$

where,

$$X_{sum} = 1/2[\{(\cos\lambda l + \cos(h_1+h_2)\lambda l)\sum_{i=1}^{q}(\cos(h_1+h_2)\lambda l_i - \cos\lambda l_i)$$
$$-(\sin\lambda l + \sin(h_1+h_2)\lambda l)\sum_{i=1}^{q}(\sin\lambda l_i + \sin(h_1+h_2)\lambda l_i)\}\times(\sin\lambda l\cos(h_1+h_2)\lambda l - \cos\lambda l\sin(h_1+h_2)\lambda l)^{-1}] \tag{3.21a}$$

Again it can be expressed for uniform pressure at the interface as given below;

$$u_r(x,t) = \alpha(\Delta u_1 + \Delta u_2) = \alpha\{(h_1 + h_2)\tan[dy(x,t)/dx]\} \tag{3.22}$$

3.4 Theoretical analysis for beam with non-uniform pressure distribution at the interfaces

3.4.1 Pressure distribution at the jointed interfaces

When a layered jointed structure is clamped together with the help of fasteners such as bolts, they come in contact at their interfaces. Under such circumstances, the interface pressure distribution profile takes a vital role for the calculation of damping capacity.

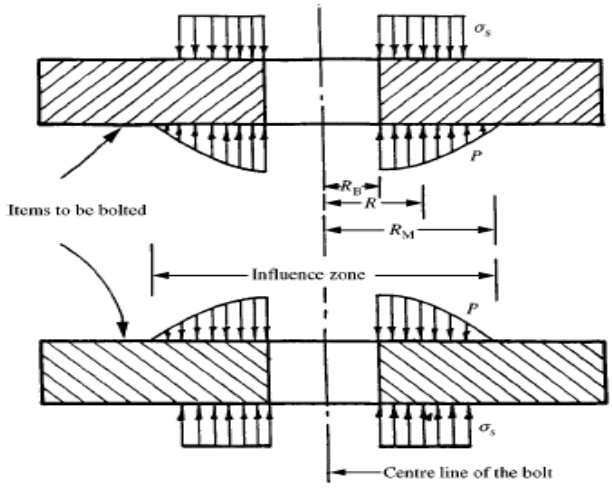

Fig.3.3 Free body diagram of a bolted joint
showing the parabolic influence zone

Moreover, it is very important to know the actual profile of interface pressure distribution and its magnitude along the beam surface for the actual assessment of the damping capacity in a jointed structure. This interface pressure originates due to the clamping action of the bolts to the cantilever beam structure.

It has been established by the researchers in the previous chapter that when two or more members are clamped with the help of bolts, a circle of contact will be formed around the bolt head with a separation taking place at a certain distance from the bolt hole as shown in Fig. 3.3.

Due to the tightening effect of the bolts on the cantilever beam the interface pressure is generated at the interfaces. The profile nature and magnitude of this interface pressure is very vital for the correct assessment of the vibration energy loss in the whole system.

It has been established in the previous chapter that the contact pressure at the interface is non-uniform in nature. It is maximum at the surface of the bolt hole and decreases with the distance away from the centre of the bolt hole. Gould and Mikic [19] and Ziada and Abd [50] have shown that the interface pressure influence zone is parabolic in nature and the influence zone is of a circle shape with 3.5 times the diameter of the connecting bolt which is independent of the tightening load applied on it. Again this has been shown by Minakuchi et al. [31] that the magnitude of interface pressure changes with the use of different thickness ratio of the beams. In the present investigation the pressure curve data of Minakuchi et al. [31] has been considered.

3.4.1.1. Determination of Non-uniform pressure distribution at the interface

The interface pressure distribution under each bolt for layered and jointed structures taken in a non-dimensional polynomial form is assumed as;

$$p/\sigma_s = C_1\left(R/R_B\right)^{10} + C_2\left(R/R_B\right)^{8} + C_3\left(R/R_B\right)^{6} + C_4\left(R/R_B\right)^{4} + C_5\left(R/R_B\right)^{2} + C_6 \qquad (3.23)$$

where p, σ_S, R and R_B are the interface pressure, surface stress on the jointed beam due to bolting, any radius within the influencing zone and radius of the connecting bolts, respectively. The surface stress σ_s depends upon the initial tension on the bolt (P) and the area under a bolt head ($A^{'}$) and is evaluated from the relation $\sigma_s=P/A^{'}$. The polynomial constants C_1, C_2, C_3, C_4, C_5 and C_6 are evaluated from the numerical data of Minakuchi et al. [31] using MATLAB software for different thickness ratios and are given in the Table-3.1 below.

The above Eq. (3.23) is a tenth order even function. This signifies that pressure profile is alike on both the sides of the bolt along the cantilever length. Moreover, the pressure is a function of the distance from the centre of the bolts. The interface pressure is maximum at the centre of the hole and gradually decreases from the centre of hole. Damisa et al. [11] have used linear pressure profile in their analysis as an approximation. But a higher order polynomial for non-uniform and uniform interface pressure distribution has been used in the present investigation in order to obtain a good accuracy.

Table 3.1 Values of constants in pressure distribution function

Polynomial constants	Ratio h_2/h_1=1.0	Ratio h_2/h_1=1.5	Ratio h_2/h_1=2.0
C_1	1.4581e-06	-1.7372e-07	-7.4198e-08
C_2	-5.7952e-05	1.3988e-05	7.4508e-06
C_3	0.60446e-03	-0.45881e-03	-0.29801e-03
C_4	0.30853e-02	0.81702e-02	0.62165e-02
C_5	-0.95814e-01	-0.87733e-01	-0.74592e-01
C_6	0.53778e+00	0.48833e+00	0.46039e+00

Table 3.2 Distance between centres of two consecutive bolts at different thickness ratios for non-uniform pressure at the interface

Thickness ratio	Ratio h_2/h_1=1.0	Ratio h_2/h_1=1.5	Ratio h_2/h_1=2.0
Distance between consecutive bolts	4.1*Dia. of bolt	4.8*Dia. of bolt	5.5*Dia. of bolt

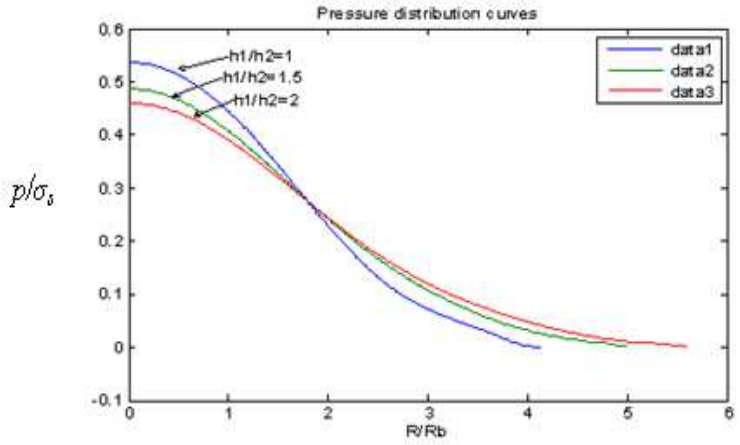

Fig.3.4 Variation of Pressure distribution (P/σ_s) for different thickness ratio at different distance (R/R_B)

Table 3.1 gives the values of the polynomial constants are different for different thickness ratios of the layered beams. This signifies that the pressure distribution varies and depends upon the thickness ratio of the layered beam. Again Table 3.2 shows the values of the distance between the centres of the consecutive bolts are

different for different thickness ratios for layered beams for non-uniform thickness ratio.

The pressure distribution curves as given by Minakuchi et al. [31] and obtained by MATLAB curve-fitting software are shown in Fig 3.4 for different thickness ratios. It presents a cumulative plot showing the variation of pressure distribution at the interfaces of the jointed beams with different thickness ratios.

The surface stress (σ_s) is rewritten as the ratio between the axial load (P) and area under the connecting bolt head (A') as shown in Fig 3.5 and is given by;

$$\sigma_s = \frac{P}{A'} = P \Big/ 3\pi R_B^2 \tag{3.24}$$

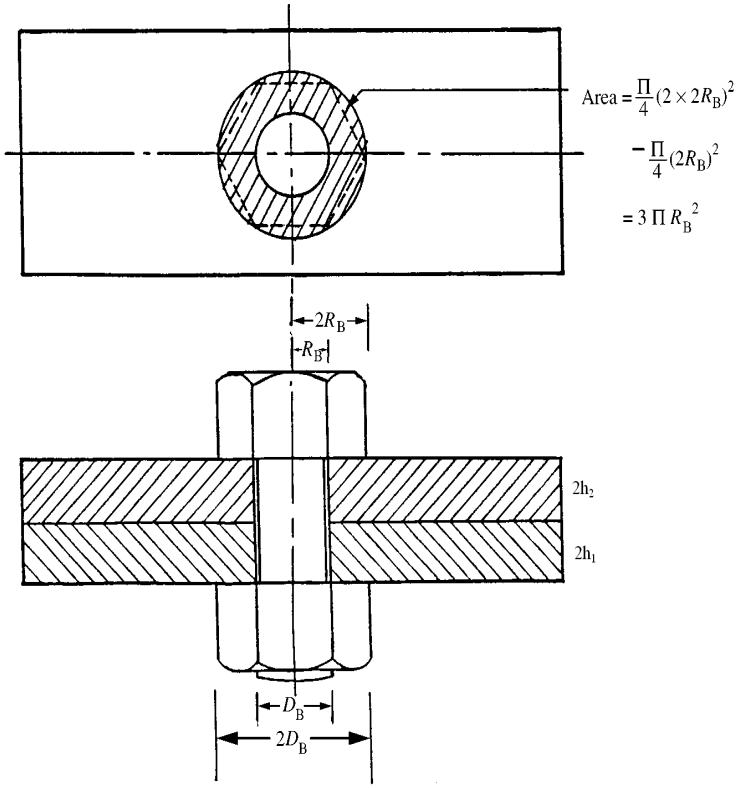

Fig.3.5 Influence area under the bolt head

Putting the value of σ_s in Eq. (3.23), the non-uniform intensity of pressure for thickness ratio 1.0 with point of separation (R/R_B), 4.1 times the diameter of bolt is found to be;

$$p = 0.00806P \Big/ 3\pi R_B^2 \qquad h_2 / h_1 = 1.0 \tag{3.25a}$$

Moreover, the intensity of pressure distribution for thickness ratio of 1.5 and 2.0 are evaluated as;

$$p = 0.00640P \Big/ 3\pi R_B^2 \qquad h_2/h_1 = 1.5 \tag{3.25b}$$

$$p = 0.00280P \Big/ 3\pi R_B^2 \qquad h_2/h_1 = 2.0 \tag{3.25c}$$

If T is the tightening torque applied on the connecting bolt, the axial load on the bolt (P) is given by Shigley [43] as;

$$P = \frac{T}{0.2D_B} \tag{3.26}$$

Putting this value of axial load in the Eqs. (3.25a), (3.25b) and (3.25c) we get;

$$p = 0.002140T \Big/ R_B^3 \qquad h_2/h_1 = 1.0 \tag{3.27a}$$

$$p = 0.001696T \Big/ R_B^3 \qquad h_2/h_1 = 1.5 \tag{3.27b}$$

$$p = 0.0007427T \Big/ R_B^3 \qquad h_2/h_1 = 2.0 \tag{3.27c}$$

3.4.2 Energy dissipation due to friction and micro slip

In structural members such as riveted and bolted; the joints are considered as the main source of energy dissipation. During transverse vibration, a jointed beam oscillates about its mean position in the transverse direction. Due to this relative motion, heat will also be generated at the interfaces, resulting in the energy loss. Sometimes friction produces defects in the structure, but in many place it can also be used for the enhancement of the damping property of the structure.

Determination of energy dissipation per cycle of vibration for non-uniform pressure distribution

The energy loss due to friction (E_f) at the interfaces for non-uniform interface is found by Nishiwaki et al. [39] to be;

$$E_f = \oint F_r \, du_r = 2 F_{rM} \, u_{rM} \tag{3.28}$$

where F_{rM} and u_{rM} are the maximum frictional force and relative dynamic slip between the interfaces at the maximum amplitude of vibration as shown in Fig.3.6 respectively.

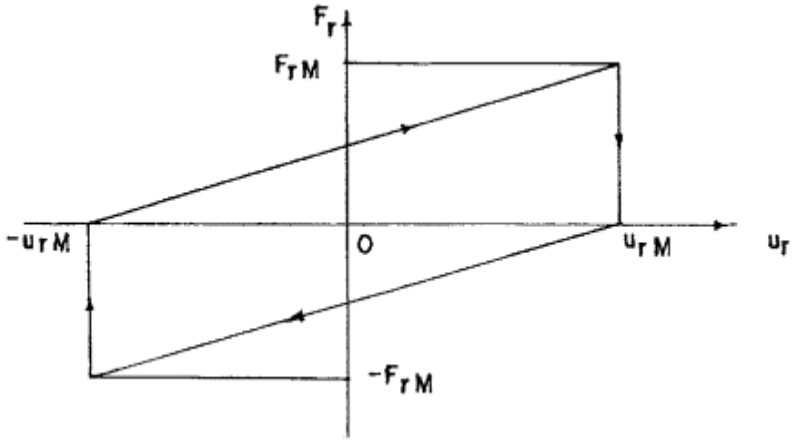

Fig.3.6 Relationship between the frictional force (F_r) and relative dynamic slip(u_r) during one cycle.

The maximum frictional force (F_{rM}) at the interfaces of the beam due to vibration is given by;

$$F_{rM} = \mu N \tag{3.29}$$

where μ and N are the kinematics coefficient of friction and total normal force at the interfaces respectively.

The normal force on an elemental circular strip of radius R and thickness dR is given by;

$$dN = p \times dA = 2p\pi R dR$$

Hence, the total normal force at the interfaces under each connecting bolt is given by;

$$N = 2\pi \int_{R_B}^{R_M} pR dR$$

$$= 2\pi \int_{R_B}^{R_M} \left[C_1 \left(R/R_B \right)^{10} + C_2 \left(R/R_B \right)^{8} + C_3 \left(R/R_B \right)^{6} + C_4 \left(R/R_B \right)^{4} + C_5 \left(R/R_B \right)^{2} + C_6 \right] \times \left[P / 3\pi R_B^2 \right] R dR$$

$$\Rightarrow N = P / 3\{(C_1 / 6)[(R_M / R_B)^{12} - 1] + (C_2 / 5)[(R_M / R_B)^{10} - 1]$$
$$+ (C_3 / 4)[(R_M / R_B)^{8} - 1] + (C_4 / 3)[(R_M / R_B)^{6} - 1]$$
$$+ (C_5 / 2)[(R_M / R_B)^{4} - 1] + C_6[(R_M / R_B)^{2} - 1]\} \tag{3.30}$$

where R_M is the limiting radius of the influencing zone under each connecting bolt. The initial tension P is the total tightening force on the bolt with which the bolts are tightened to the beam layers. This total force is be expressed as,

$$P = \frac{T}{0.2 D_B}$$

Finally Eq. (3.28) for energy dissipation per cycle of vibration is obtained by putting the value of F_{rM} and u_{rM} from Eq. (3.29) and (3.21) respectively, we get;

$$E_f = 2\left[(\mu N) \times \frac{1}{2} (\alpha (h_1 + h_2) X_{sum} \lambda y(l, 0)) \right] \tag{3.31}$$

Simplifying the above Equation, we can rewrite the total energy loss due to friction as;

$$E_f = \mu \alpha N (h_1 + h_2) X_{sum} \lambda y(l, 0) \tag{3.32}$$

3.4.3 Determination of logarithmic decrement (δ)

Logarithmic damping decrement is used as a measure of damping capacity of a lightly damped structure and is influenced by relative dynamic slip and interface pressure at the surface of contact. The logarithmic damping decrement, δ, is usually expressed as the ratio between two consecutive amplitudes of a same cycle. This approach is generally used to estimate the damping capacity from the experiments in which the decay of amplitude is recorded from the storage oscilloscope signals. The logarithmic damping decrement is usually expressed as,

$$\delta = \frac{1}{n} \ln \left(\frac{a_n}{a_{n+1}} \right) \tag{3.33}$$

where, a_n is the amplitude of vibration at nth cycle and a_{n+1} is the amplitude of vibration at the (n+1)th cycle.

In the present investigation for the theoretical evaluation of damping, the energy approach is used, because the logarithmic decrement is fundamentally equal to the energy loss per cycle of vibration. Nishiwaki et al. [38] have presented that the logarithmic decrement depends on both the energy loss (E_{loss}) and energy stored (E_{ne}) in a system during one cycle of vibration. Thus, the logarithmic decrement is expressed as;

$$\delta = \frac{1}{2}(E_{loss} / E_{ne}) \tag{3.34}$$

The energy introduced into the layered and jointed cantilever beam in the form of strain energy per half-cycle of vibration is given by;

$$E_{ne} = \left(3EI/l^3\right) y^2 (l,0) \tag{3.35}$$

Replacing $3EI/l^3=k$, i.e., the static bending stiffness of the layered and jointed beam, in Eq. (3.35), the energy introduced into the system can be written as;

$$E_{ne} = ky^2 (l,0) \tag{3.36}$$

3.4.3.1 Logarithmic decrement (δ) for non-uniform pressure

The energy loss (E_{loss}) in a structural system usually consists of the sum of the energy loss (E_f) due to friction at the joints and the energy loss (E_0) due to the material and support of the structure itself. Therefore, the logarithmic decrement (δ) of a jointed cantilever beam is expressed as;

$$\delta = \frac{1}{2}\left(\frac{E_f}{E_{ne}}\right) + \frac{1}{2}\left(\frac{E_0}{E_{ne}}\right) = \delta_f + \delta_0 \tag{3.37}$$

where δ_f is the logarithmic damping decrement due to friction and δ_0 the logarithmic damping decrement due to material and support of the structure.

The energy loss may arise due to joints, material and support damping. However the main source that was assumed by researchers is the slip and friction at the joints, because the material and support damping value is much more less than the friction damping value. Therefore, the term δ_0 in the above equation is neglected; the logarithmic decrement is theoretically evaluated from the energy loss arising from the friction only. Due to this assumption Eq. (3.37) can be rewritten as;

$$\delta \approx \delta_f = (E_f / 2E_{ne}) \tag{3.38}$$

Finally substituting the values of E_f and E_{ne} as presented in Eqs. (3.32) and (3.36), respectively, in Eq. (3.38), the logarithmic decrement is finally expressed as;

$$\delta = [\mu\alpha N(h_1 + h_2) X_{SUM} \lambda] / ky(l,0) \tag{3.39}$$

3.4.4 Determination of product of μα

The energy dissipation depends upon many factors such as the thickness, width and the interface pressure of the beam. However it mainly depends upon the kinematic coefficient of friction (μ) and dynamic slip ratio (α) at the interfaces. Since it is very difficult to assess the damping produced in the joints due to variations of the above two vital parameters under dynamic loading conditions, their product ($\mu\alpha$) is taken as a constant for a particular specimen irrespective of the surface condition. Thus, this product, $\mu\alpha$, *is* found out modifying Eq. (3.39) for non-uniform interface pressure as given below;

$$\mu\alpha = \frac{ky\,(l,0)\,\delta}{N\,(h_1 + h_2)\,X_{sum}\,\lambda} \tag{3.40}$$

3.5 Theoretical analysis for bolted beam with uniform pressure distribution at the interfaces

3.5.1 Determination of Uniform pressure distribution at the interface

The interface pressure distribution under each bolt is assumed as a non-dimensional polynomial of parabolic shape for layered and jointed structures. In order to get uniform pressure distribution at the interfaces, the adjoining interface pressures are superimposed by reducing the distance between the centers of the consecutive bolts as shown in the Fig.3.7. The optimum distance between the consecutive bolts for attaining uniform pressure condition at the interface is found out using MATLAB software as given in Table 3.3

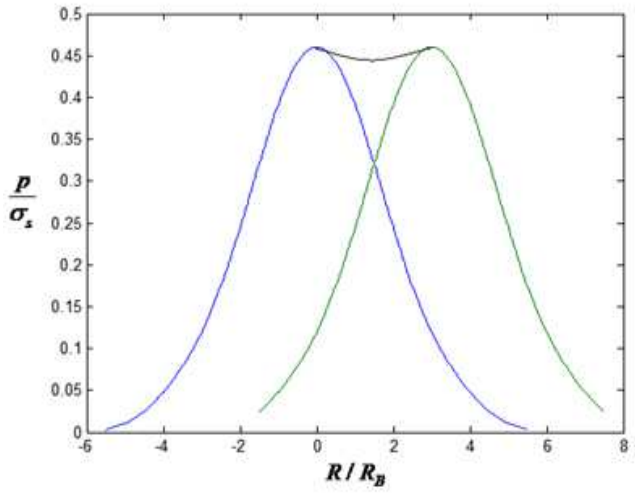

Fig.3.7 Uniform pressure distribution of bolted joints by reducing the distance between consecutive bolts

Table.3.3 Distance between the centers of two consecutive bolts at different thickness ratios for uniform pressure at the interfaces.

Thickness ratio	Ratio h_2/h_1=1.0	Ratio h_2/h_1=1.5	Ratio h_2/h_1=2.0
Distance between consecutive bolts	2.336*Dia. of bolt	2.401*Dia. of bolt	2.410*Dia. of bolt

Putting the value of distance between two consecutive bolts from the above Table 3.3 and the value of σ_s in the Eq. (3.23), the equation for thickness ratio 1.0 with point of separation 2.336 for uniform pressure is rewritten as;

$$p = 0.39474P \Big/ 3\pi R_B^2 \qquad h_2/h_1 = 1.0 \tag{3.41a}$$

The intensity of pressure distribution for thickness ratio of 1.5 and 2.0 are also evaluated as;

$$p = 0.40583P \Big/ 3\pi R_B^2 \qquad h_2/h_1 = 1.5 \tag{3.41b}$$

$$p = 0.41156P \Big/ 3\pi R_B^2 \qquad h_2/h_1 = 2.0 \tag{3.41c}$$

Putting the value of axial load *P* from Eq. (3.26) in Eqs. (3.41a), (3.41b) and (3.41c), the final value of interface pressure for thickness ratio 1.0, 1.5 and 2.0 are rewritten as;

$$p = 0.10471T \Big/ R_B^3 \qquad h_2/h_1 = 1.0 \tag{3.42a}$$

$$p = 0.10765T \Big/ R_B^3 \qquad h_2/h_1 = 1.5 \tag{3.42b}$$

$$p = 0.10917T \Big/ R_B^3 \qquad h_2/h_1 = 2.0 \tag{3.42c}$$

3.5.2 Determination of energy dissipation per cycle of vibration for uniform pressure distribution

As discussed earlier, the energy is dissipated due to the relative dynamic slip at the interfaces in a jointed structure.

For the above cantilever beam of length l and height $2h_1+2h_2$ as shown in Fig. 3.2, the interface pressure at x is expressed as $p(x)$ and the normal load acting on the length of dx is $p(x)bdx$, where b is the width of beam.

Thus, the frictional force at the interfaces is given by;

$$F = \mu p(x) b dx \tag{3.43}$$

where μ is the coefficient of kinematic friction.

By considering the condition that the interface pressure is uniformly spread all over the contact area, $p(x)$ yields p. For the above cantilever beam with uniform pressure distribution at the interfaces, p, and the energy loss due to the frictional force at the interfaces per half-cycle of vibration is given by;

$$E_{loss} = \int_0^{\pi/\omega_n} \int_0^{l} \mu p b \left[\left\{ \partial u_r (x,t) / \partial t \right\} dx dt \right] \tag{3.44}$$

However, the energy introduced into the layered and jointed cantilever beam in the form of strain energy per half-cycle of vibration is given by;

$$E_{ne} = \left(3EI / l^3 \right) y^2 (l,0) \tag{3.45}$$

where E, $I = b(2h_1 + 2h_2)^3 / 12$ and $y(l,0)$ are the modulus of elasticity, cross-sectional moment of inertia and transverse deflection at the free end of the beam, respectively.

From the above equations (3.44) and (3.45), the ratio of energy is found to be;

$$\frac{E_{loss}}{E_{ne}} = \left[\mu b p \alpha (h_1 + h_2) \Big/ \left\{ \left(3EI / l^3 \right) y^2 (l,0) \right\} \right] \int_0^{\pi/\omega_n} \int_0^{l} \left[\frac{\partial}{\partial t} \left\{ \tan \partial y(x,t) / \partial x \right\} \right] dx dt \tag{3.46a}$$

The slope of the cantilever beam $\partial y(x,t)/\partial x$ being very small is modified as; $\tan(\partial y(x,t)/\partial x) \simeq \partial y(x,t)/\partial x$. Therefore, the ratio of energy can be rewritten as;

$$\frac{E_{loss}}{E_{ne}} = \left[\frac{\mu b p \alpha (h_1 + h_2)}{\left\{ \left(3EI / l^3 \right) y^2 (l,0) \right\}} \right] \int_0^{\pi/\omega_n} \int_0^{l} \left\{ \partial^2 \left(y(x,t) \right) / \partial x \partial t \right\} dx dt \tag{3.46b}$$

On integrating the equation (3.46b) and simplifying ratio of energy is found to be;

$$\frac{E_{loss}}{E_{ne}} = \left[\frac{\mu bp\alpha (h_1 + h_2)}{\left\{ \left(3EI/l^3 \right) y^2 (l,0) \right\}} \right] y(l,0) \tag{3.46c}$$

Finally ratio of energy is given by;

$$\frac{E_{loss}}{E_{ne}} = \frac{\mu bp\alpha (h_1 + h_2)}{\left(3EI/l^3 \right) y(l,0)} \tag{3.47}$$

The damping capacity, ψ, is expressed as the ratio of energy dissipated due to the relative dynamic slip at the interfaces and the total energy introduced into the system and is found to be;

$$\psi = \left[E_{loss} / \left(E_{loss} + E_{ne} \right) \right] = 1 / \left[1 + E_{ne} / E_{loss} \right] \tag{3.48}$$

Replacing $3EI/l^3=k$, i.e., the static bending stiffness of the layered and jointed beam, the damping capacity is found out from expressions (3.47) and (3.48) as;

$$\psi = \frac{1}{1 + \left[ky(l,0) \right] / \left[2\mu bp\alpha (h_1 + h_2) \right]} \tag{3.49}$$

3.5.3 Logarithmic decrement (δ) for uniform pressure

Assuming that the energy stored in the system is proportional to the square of the corresponding amplitude, the relationship between logarithmic damping decrement and damping capacity can be written as;

$$\delta = \frac{1}{2} \ln \left(1 / (1 - \psi) \right) \tag{3.50}$$

Putting the expression of damping ratio in expression (3.50) and simplifying we get;

$$\delta = \frac{1}{2} \ln \left[\frac{2\mu\alpha bp(h_1 + h_2)}{ky(l,0)} + 1 \right] \tag{3.51}$$

3.5.4 Determination of product of $\mu\alpha$

The product of μα is also assumed to be constant for uniform pressure distribution at the interfaces and is given by,

$$\mu\alpha = \frac{ky(l,0)\left[e^{2\delta} - 1 \right]}{2bp(h_1 + h_2)} \tag{3.52}$$

3.6 Chapter summary

This chapter gives a detailed solution for the parameters that are affecting the transverse vibration of a beam structure. In the present work Euler-Bernoulli beam theory is adopted. Further, the relative dynamic slip at the interfaces has been evaluated for both non-uniform and uniform pressures at the interface. Again the interface pressure distribution has been determined and same is found to be parabolic in nature [32, 50], being maximum at the bolt hole and decreasing gradually away from the bolt. Further, the logarithmic decrements, for both the uniform and non-uniform interface pressure, in case of two and multilayered beams jointed with bolts, have been derived. Moreover, the damping capacity of cantilever beams with different thickness ratios has been evaluated theoretically. It is established that the damping capacity is mainly affected by various factors such as, thickness ratio, length, width of beam, diameter of bolt, interface pressure distribution, etc. Therefore, a detailed study on all the above vital parameters has been carried out in the present analysis.

CHAPTER-4

EXPERIMENTAL ANALYSIS

4.1 Introduction

In the previous chapter, the classical approach is applied for predicting the damping in layered and bolted cantilever beams. In order to find out the damping capacity of jointed beams experimentally and compare it with the theoretical results, an experimental set-up with a number of specimens has been fabricated as shown in Figs 4.1 to 4.4 with detailed instrumentation. The specimens are prepared from commercial mild steel flats by joining two and more numbers of layers with varying thickness ratios of 1.0, 1.5 and 2.0 by bolts as shown in Tables 4.1-Table 4.7.

4.2 Preparation of specimens

The test specimens of different sizes are prepared from the same stock of commercial mild steel flats as presented in Tables 4.1 to 4.7 for non-uniform and uniform pressure at the interfaces. Equi-spaced bolts of diameter 12 mm are used to fabricate two and multi layered specimens with different tightening torque. The tightening torque of bolts is varying from 3.46, 6.92, 10.38, 13.84, 17.3, 20.76, 24.22 and 27.68 Nm (i.e., 2.50, 5.00, 7.50, 10.00, 12.50, 15.00, 17.50 and 20.00 lb ft respectively). For all non-uniform interface pressure specimens, the distance between the consecutive bolts is so arranged that their influence zone just touches each other at the point of separation. Moreover for all uniform interface pressure specimens their influence zone overlaps with each other or reduced to attain uniform pressure. The width and length of the specimens are also interchanged with respect to the bolt diameter and beam thickness ratio as per the zone of influence.

For considering non-uniform interface pressure, the distance between the centers of the consecutive bolts and the width of the beam are kept as 4.1, 4.8 and 5.5 times the diameter of the bolt for thickness ratios 1.0, 1.5 and 2.0, respectively. Again, for considering uniform interface pressure, the distance between the centers of the consecutive bolts and the width of the beam are kept as 2.336, 2.402 and 2.410 times the diameter of the bolt for thickness ratios 1.0, 1.5 and 2.0, respectively.

The tightening torque on the bolts is kept uniform for a set of experiments. The cantilever beam lengths have been varied as per the zone of influence. Also the

diameters of bolt have been varied for different beam lengths. Photographs of two of the specimens used in the experiments are presented in Figs 4.1 and 4.2.

Fig.4.1 Two layered mild steel bolted test specimen

Fig.4.2 Four layered mild steel bolted test specimen

Table.4.1. Details of mild steel bolted specimens for non-uniform pressure with thickness ratio 1.0

No of layers	Dimension of the specimen width×$(2h_1+2h_2)$ (mm)	Diameter of the connecting bolt (mm)	Number of bolts Used	Length of beam (mm)
2	49.2 ×(2+2)	12	6 7 8	295.2 344.4 393.6
	49.2 × (3+3)	12	6 7 8	295.2 344.4 393.6
	49.2 × (4+4)	12	6 7 8	295.2 344.4 393.6

Table.4.2. Details of mild steel bolted specimens for non-uniform pressure with thickness ratio 1.5

No of layers	Dimension of the specimen width×($2h_1$+$2h_2$) (mm)	Diameter of the connecting bolt (mm)	Number of bolts used	Length of beam (mm)
2	57.6 × (2+3)	12	6 7 8	345.6 403.2 460.8
	57.6 × (3+4.5)	12	6 7 8	345.6 403.2 460.8
	57.6× (4+6)	12	6 7 8	345.6 403.2 460.8

Table.4.3. Details of mild steel bolted specimens for non-uniform pressure with thickness ratio 2.0

No of layers	Dimension of the Specimen width×($2h_1$+$2h_2$) (mm)	Diameter of the connecting bolt (mm)	Number of bolts used	Length of beam (mm)
2	66 × (2+4)	12	6 7 8	396 462 528
	66 × (3+6)	12	6 7 8	396 462 528
	66 × (4+8)	12	6 7 8	396 462 528

Table.4.4. Details of mild steel bolted two layers specimens for uniform pressure with thickness ratio 1.0

No of layers	Dimension of the specimen width×($2h_1$+$2h_2$) (mm)	Diameter of the connecting bolt (mm)	Number of bolts used	Length of beam (mm)
2	28.036× (2+2)	12	13	364.468
			12	336.432
			11	308.396
	28.036× (3+3)	12	13	364.468
			12	336.432
			11	308.396
	28.036× (4+4)	12	13	364.468
			12	336.432
			11	308.396

Table.4.5. Details of mild steel bolted multi-layered specimens for uniform pressure with thickness ratio 1.0

No of layers	Dimension of the specimen width×($2h_1$+$2h_2$) (mm)	Diameter of the connecting bolt (mm)	Number of bolts used	Length of beam (mm)
3	28.036× (2+2+2)	12	13	364.468
			12	336.432
			11	308.396
	28.036× (3+3+3)	12	13	364.468
			12	336.432
			11	308.396
	28.036× (2+2+2+2)	12	13	364.468
			12	336.432
			11	308.396
4	28.036× (3+3+3+3)	12	13	364.468
			12	336.432
			11	308.396

Table.4.6. Details of mild steel bolted specimens for uniform pressure with thickness ratio 1.5

No of layers	Dimension of the specimen width×($2h_1$+$2h_2$) (mm)	Diameter of the connecting bolt (mm)	Number of bolts used	Length of beam (mm)
2	28.812× (2+3)	12	13	374.556
			12	345.744
			11	316.932
	28.812× (3+4.5)	12	13	374.556
			12	345.744
			11	316.932
	28.824× (4+6)	12	13	374.556
			12	345.744
			11	316.932

Table.4.7. Details of mild steel bolted specimens for uniform pressure with thickness ratio 2.0

No of layers	Dimension of the specimen width×($2h_1$+$2h_2$) (mm)	Diameter of the connecting bolt (mm)	Number of bolts used	Length of beam (mm)
2	28.92× (2+4)	12	13	375.96
		12	12	347.04
		12	11	318.12
	28.92× (3+6)	12	13	375.96
		12	12	347.04
		12	11	318.12

4.3 Description of the experimental set-up

The schematic of the experimental set-up with the detailed instrumentation and photographic views are shown in Figs 4.3 and 4.4, respectively. The set-up consists of welded fabricated structure of steel channels. The frame is grouted on a heavy and rigid concrete base by means of foundation bolts. The frame has the provision of slotted guide ways to hold the beams of different lengths. The photographic view of

the experimental set-up with clamping arrangement at the base of cantilever beam and the photographic view of the experimental set up with spring loaded exciter and dial gauge arrangement are shown in Figs 4.5 and 4.6 respectively.

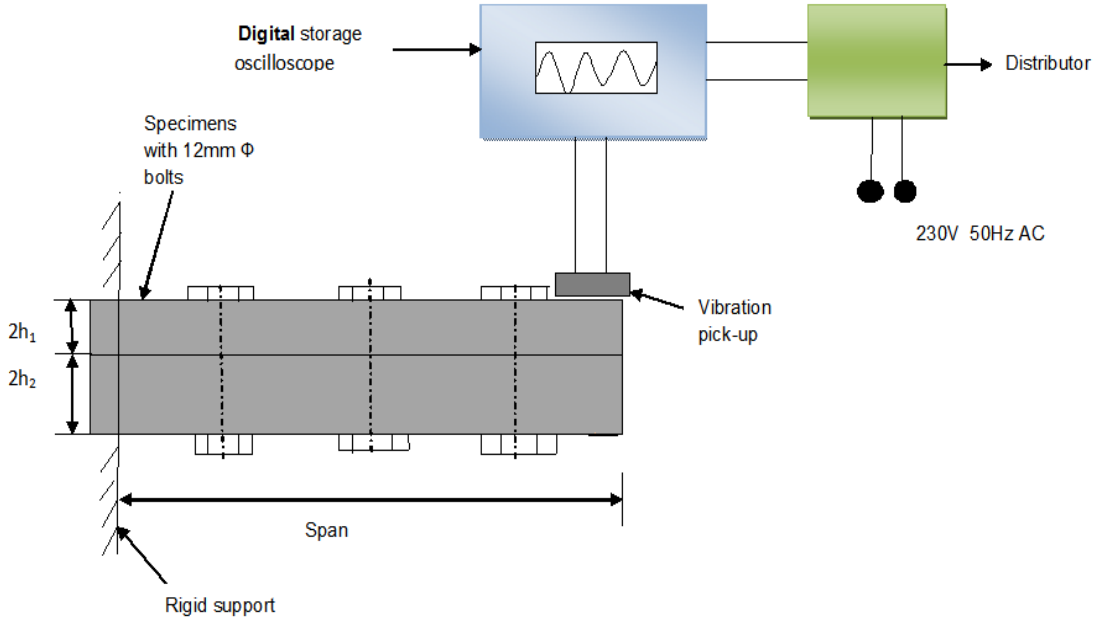

Fig.4.3 Schematic of the experimental set-up

The frame has the provision at both the sides to hold the cantilever beam specimens tightly and rigidly in order to ensure perfect cantilever condition. The beam specimen can be clamped with the help of a screw jack type vice. The base plate and the handle of the clamp prevent the rotation of the specimens while applying load at the fixed end. For initiating the vibration at the free end of the specimens with low amplitudes a spring loaded exciter is used. One dial gauge is attached to the frame which is used to calibrate the reading of the initial amplitudes of excitation. The dial gauge is mounted to a vertical stand with a magnetic base. A contacting type of vibration pick-up is attached to the beam, which senses the free vibration of the specimen and the corresponding signal is fed to a digital storage oscilloscope to obtain a steady signal. The logarithmic damping decrement is then evaluated from the stored amplitudes of the digital storage oscilloscope.

Fig.4.4 Photographic view of the experimental set-up

Fig. 4.5 Side view of experimental setup
showing clamping arrangement

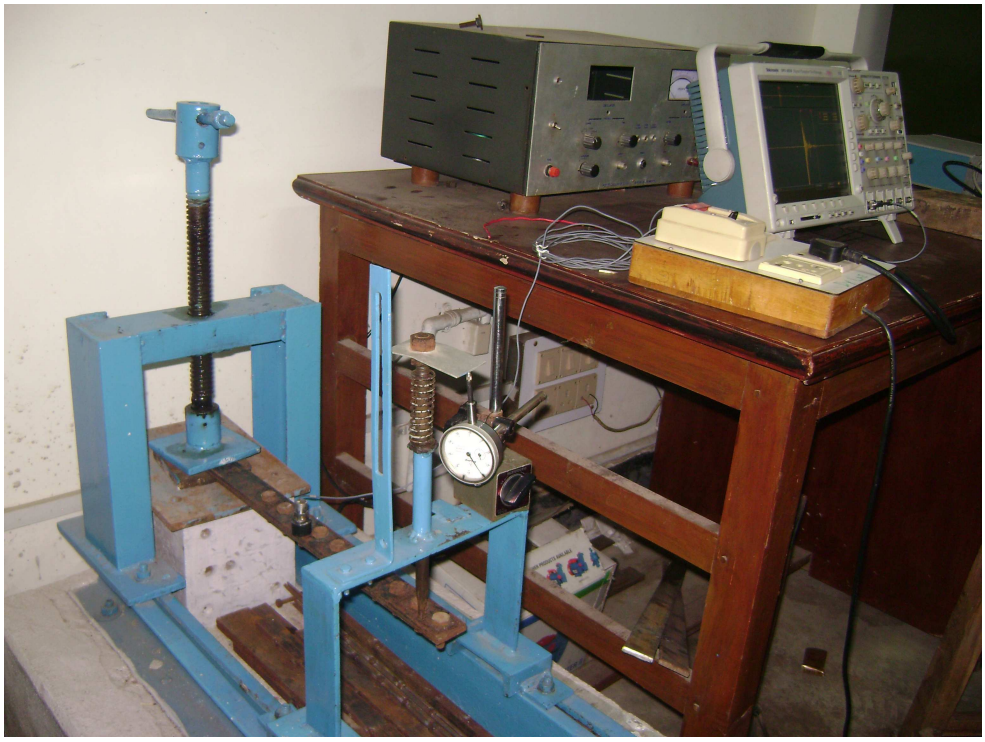

Fig. 4.6 Photographic view of the spring loaded exciter with a dial gauge

The experimental set up consists of instruments, such as;

- Digital storage oscilloscope
- Contacting type vibration pick-up
- Dial gauge
- Distributor box

Digital storage oscilloscope

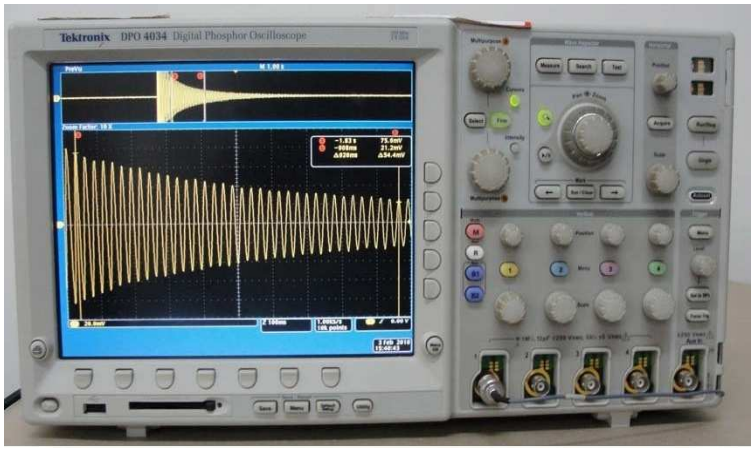

Fig.4.7 Digital storage oscilloscope

A digital storage oscilloscope is a type of electronic instrument which is used for processing and displaying vibration signals. As shown in Fig. 4.5, a digital oscilloscope contains various input connectors, control buttons on the panel to adjust the instrument to get the exact value of signals. The signal to be measured is fed to one of the connectors. It plots a two dimensional graph of the time history curve.

Specifications:

Tektronix 4000 series
DPO 4000 series Oscilloscope
Input Voltage: 100 V to 240 V ± 10%
Input Power Frequency: 47 Hz to 66 Hz (100 V to 240 V)
400 Hz (100 V to 132 V)
Power Consumption: 250 W maximum
Weight: 5 kg (11 lbs), standalone instrument
Clearance: 51 mm (2 in)
Temperature
Operating Temperature: 0 to 50 0C

Humidity

Operating Humidity: High: 40 to 50 0C, 10 to 60% RH
Operating Humidity: Low: 0 to 40 0C, 10 to 90% RH

Altitude

Operating: 3000 m (about 10,000 ft)
Non-operating: 12,192m (40000 ft)

Random Vibration

Operating: 0.31 G_{RMS}, 5 – 500 Hz, 10 minutes per axis, 3 axes (30 minutes total)
Non-operating: 2.46 G_{RMS}, 5-500Hz, 10 minutes per axes, 3 axes (30 minutes total)
Pollution Degree: 2, Indoor use only

Contacting type vibration pick-up

Fig.4.8 Contact type vibration pick-up

The vibration pick-up is a device that transforms the mechanical quantities, such as displacement, velocity or acceleration into electrical quantities, such as voltage or current. These are of various types such as contacting and non-contacting type. In the present work contacting type vibration pick-up is used. One end of the accelerometer is a magnetic base which is attached to the vibrating surface and the other end is connected to the first connector port of the storage oscilloscope. The accelerometer used in the experiments is shown in Fig 4.6.

Specifications:-

Type: - MV-2000.

- Dynamic frequency range: - 2 c/s to 1000 c/s
- Vibration amplitude: - ±1.5 mm max.
- Coil resistance: - 1000Ω
- Operating temperature: - 10ċ to 40 ċ
- Mounting: - by magnet
- Dimensions: - cylindrical Length:-45 mm Diameter: - 19 mm
- Weight: - 150 grams

Dial gauge

Fig.4.9 Dial gauge mounted on a stand with magnetic base

Dial gauge instruments are used for accurate measurement of a small distance. They may also be known as a Dial test indicator (DTI), or as a “clock”. They are named so because the measurement results are displayed in a magnified way by means of a dial. Dial indicator may be used to check the variation in tolerance during the inspection process of a machined part, measure the deflection of a beam under dynamic loading conditions, as well as many other situations where a small measurement needs to be indicated. The dial gauge, as shown in Fig 4.7, is shock proof and can measure the amplitude of excitation in the range of 0.01 to 20 mm.

Distributor box

A distribution box supplies the AC power to the storage oscilloscope at a voltage and frequency of 230V and 50Hz, respectively.

4.4 Testing procedure

In order to find out the damping capacity of jointed beams experimentally and compare it with the theoretical results, an experimental set-up has been fabricated. For this, experiments have been conducted on the prepared specimens. Various measurement techniques have been used for the calculation of Young’s modulus of elasticity, static bending stiffness and theoretical logarithmic decrement.

4.4.1 Measurement of Young’s modulus of elasticity

The Young’s modulus of elasticity (E) of the specimen material is found out by conducting static deflection tests. For this purpose, few samples of solid specimen beams are selected from the same stock of mild steel flats. These specimens are mounted on the same experimental set-up rigidly so as to ensure perfect boundary conditions for cantilever beam. Static loads (W) are applied at the free end and the corresponding deflections (Δ) are recorded. The Young’s modulus for the specimen material is then determined using the expression $E=WL^3/3I\Delta$, where L and I are the free length and moment of inertia of the cantilever specimen. The average of some readings is recorded from the tests from which the average value of Young’s modulus is evaluated and is found to be 198.2 GN/m^2 for mild steel specimens.

4.4.2 Measurement of static bending stiffness

The stiffness of a bolted joint beam is less than the stiffness of a solid beam. This means that the stiffness of the beam used is decreased due to joints present in the structure. The reduction in the stiffness of the structure is also called stiffness ratio.

This can be represented as the ratio of stiffness of jointed beam to that of the solid beam. The value of stiffness ratio is much more important for the actual calculation of logarithmic damping decrement. The same static deflection tests are conducted as in case of Young's modulus to measure the actual stiffness (k) of a jointed specimen using the relation $k=W/\Delta$. However, the stiffness of an identical solid cantilever mild steel beam is theoretically calculated from the expression $k'=3EI/L^3$. The average values of the stiffness ratios for two layered cantilever beams jointed with bolts has been calculated by using the above two expressions. Further, the stiffness ratio of multi-layered jointed beams has been calculated in the similar manner as in case of two layered ones for thickness ratio 1.0.

4.4.3 Measurement of logarithmic damping decrement (δ)

After finding out the Young's modulus and static bending stiffness of the specimen, tests are conducted for evaluating the logarithmic damping decrement. The specimens are rigidly mounted to the support in order to obtain perfect cantilever condition. This further ensures that any loss due to support, etc. is neglected and the damping in the system is owing to the jointed effect of the specimens.

First of all a spring loaded exciter is used to excite the specimen at the free ends. The excitation is given in a range of 0.1 to 0.5 mm amplitude. At the starting the beam is deflected and released to oscillate at its first mode of vibration. A contacting type vibration pick-up is attached to the beam gives the response of the beam when it is vibrating. The vibration pick-up is magnetically attached to the free end of the specimen and the other end is connected to the storage oscilloscope port. This output signal is fed to a digital storage oscilloscope for processing and display. The data is then analyzed to determine the natural frequency and damping characteristics of the beam structure. The signal displayed on the screen of the storage oscilloscope indicates the energy dissipation and it gradually decreases with time.

The response of the specimen is taken from the digital storage oscilloscope and it is used for the estimation of the logarithmic damping decrement by using the expression $\delta = \frac{1}{n}\ln\left(a_n / a_{n+1}\right)$, where a_n, a_{n+1} and n are the recorded values of the amplitude of the first cycle, last cycle and number of cycles, respectively. For same tightening torque the experiment is repeated for five times by changing the amplitude of excitation.

The connecting members of the test specimen are prepared in such a manner that they are flat with perfect contact at the interface. Accurate tightening torque has been applied on each bolt in order to ensure identical pressure distribution at the interface of the specimens.

4.5 Experimental evaluation of $\mu\alpha$

Damping capacity of a structure depends on various factors. The kinematic coefficient of friction (μ) and dynamic slip ratio (α) are two vital parameters which affect the energy dissipation of the structure. Normally with the increase in dynamic slip at the interfaces the coefficient of friction decreases and vice versa. It is very difficult to find out the exact value of the individual parameters at a particular condition of excitation under dynamic loading. Therefore, it is convenient to take the product $\mu\alpha$ as a single parameter from the experimental results and use it for theoretical calculations for other conditions of a particular beam specimen under a particular condition of vibration irrespective of its surface roughness.

Due to the above reason the product of $\mu\alpha$ has been determined from the experimental results of logarithmic decrement of a two layered bolted beam. By taking the values of the product $\mu\alpha$ for different frequencies graphs are plotted. These graphs are further used for the theoretical evaluation of logarithmic decrements of layered and jointed beams of different specification and conditions of excitation using Eq. (3.40) and (3.52) for classical methods, for non-uniform and uniform pressure at the interface respectively. Figs 4.8 to 4.13 show variations of $\mu\alpha$ with different tightening torque of different beams. These graphs are further used to calculate the theoretical values of logarithmic decrement of various specimens.

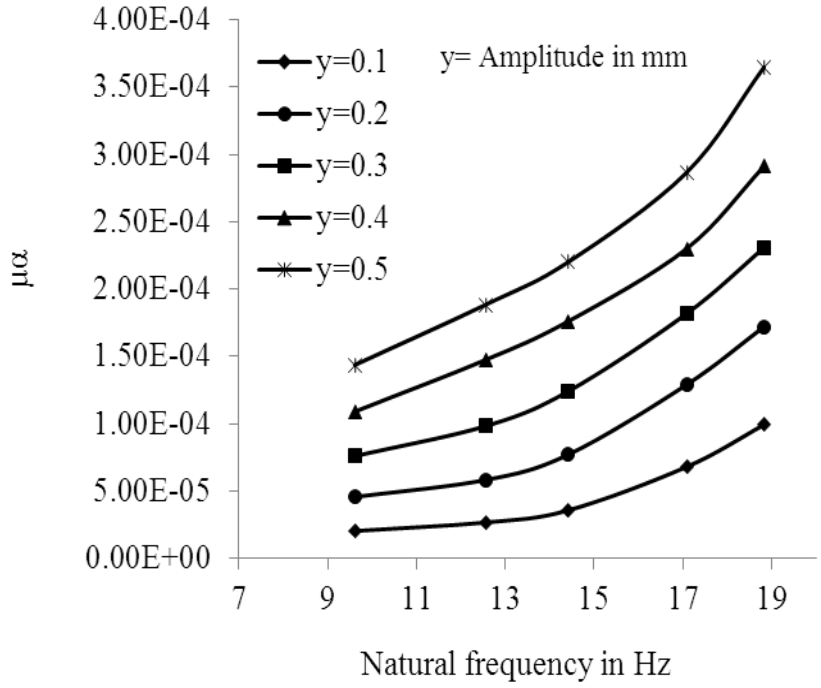

Fig.4.10 Variation of μα with Natural frequency of vibration for mild steel specimens with beam thickness ratio 1.0 at different initial amplitudes of excitation (y) for non-uniform interface pressure

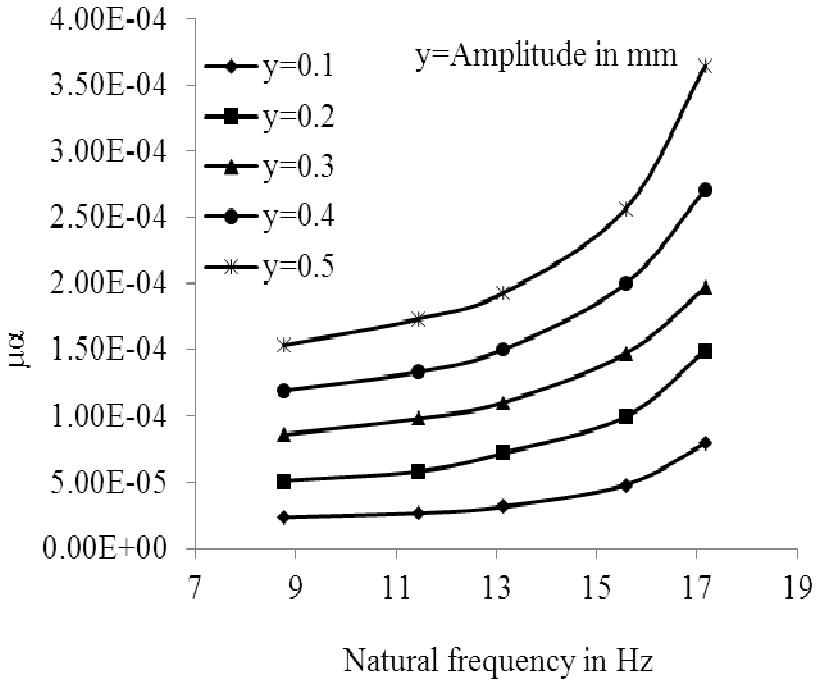

Fig.4.11 Variation of μα with Natural frequency of vibration for mild steel specimens with beam thickness ratio 1.5 at different initial amplitudes of excitation (y) for non-uniform interface pressure

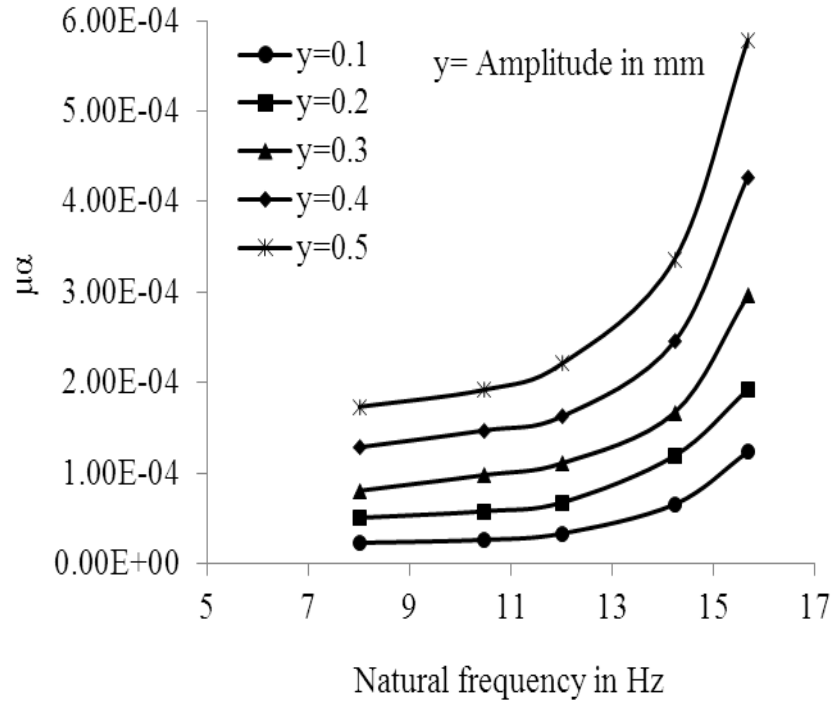

Fig.4.12 Variation of μα with Natural frequency of vibration for mild steel specimens with beam thickness ratio 2.0 at different initial amplitudes of excitation (y) for non-uniform interface pressure

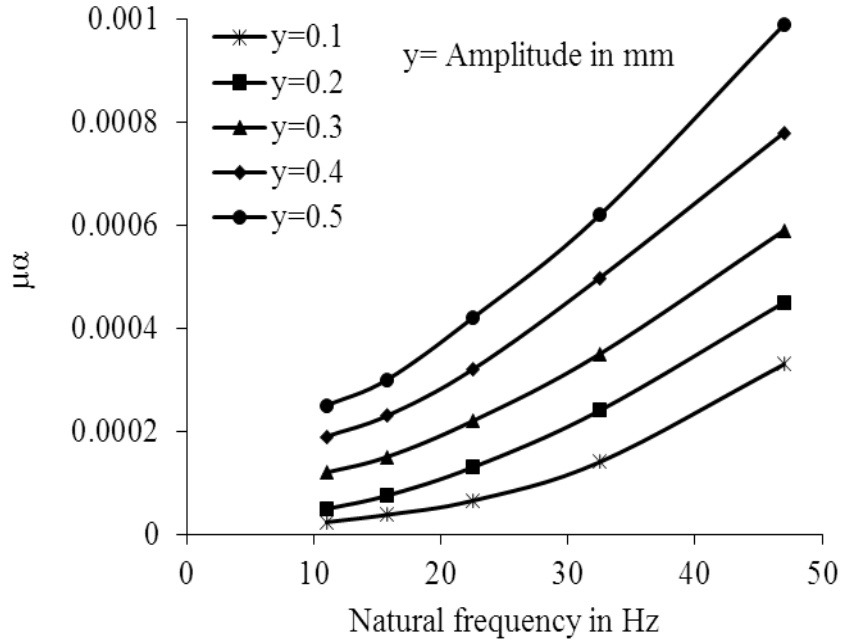

Fig.4.13 Variation of μα with Natural frequency of vibration for mild steel specimens with beam thickness ratio 1.0 at different initial amplitudes of excitation (y) for uniform interface pressure

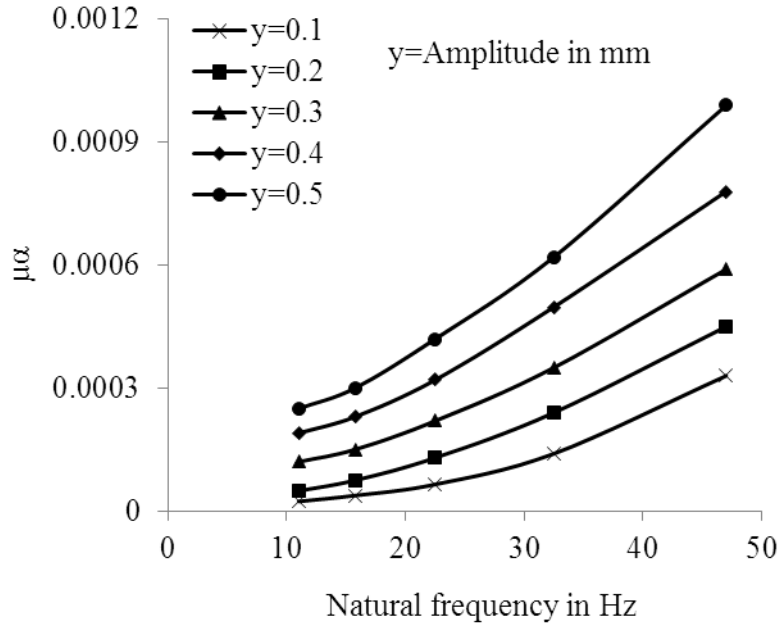

Fig.4.14 Variation of μα with Natural frequency of vibration for mild steel specimens with beam thickness ratio 1.5 at different initial amplitudes of excitation (y) for uniform interface pressure

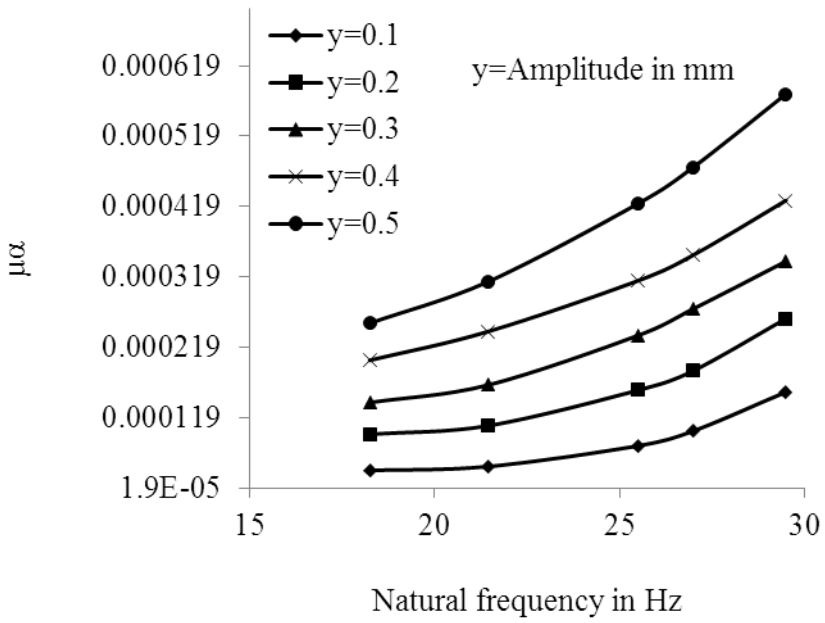

Fig.4.15 Variation of μα with Natural frequency of vibration for mild steel specimens with beam thickness ratio 2.0 at different initial amplitudes of excitation (y) for uniform interface pressure

4.6 Chapter summary

This chapter describes the detail of the experimental set-up, instrumentation, sample preparation and different testing methods that are used for the measurement of Young's modulus of elasticity, static bending stiffness and damping capacity of the specimens. The actually measured logarithmic damping decrement deviates from the theoretically computed damping capacity of a structure due to assumptions made in the theoretical analysis. For different set of layered and bolted mild steel specimens experimental results are measured in terms of logarithmic decrement using the time signals with the help of a storage oscilloscope. The same results are compared with the corresponding numerical values obtained in chapter-3 for establishing the authenticity of the theory developed. These comparative results are presented in graphical forms in chapter-5.

CHAPTER-5

RESULTS AND DISCUSSION

In order to authenticate the theory developed for damping capacity of jointed beams with various thickness ratios and bolted joints, experiments are conducted as outlined in the previous chapter and the results are compared with the theoretical ones by plotting the graphs.

The logarithmic damping decrements are found out numerically from Eq. (3.39) and Eq. (3.51) for non-uniform and uniform pressure distribution respectively using the values of the product of dynamic slip ratio and kinematic co-efficient of friction determined from the graphs as shown in Fig 4.8 to Fig 4.13 at different natural frequencies of vibration and initial amplitude of excitation. These numerical as well as the corresponding experimental results are plotted as solid (——) and dotted lines (------) respectively for comparison as shown in Figs. 5.1 to Fig 5.19. It is observed that both the curves are in good agreement with a maximum variation of 10.4% which shows the authenticity of the theoretical analysis.

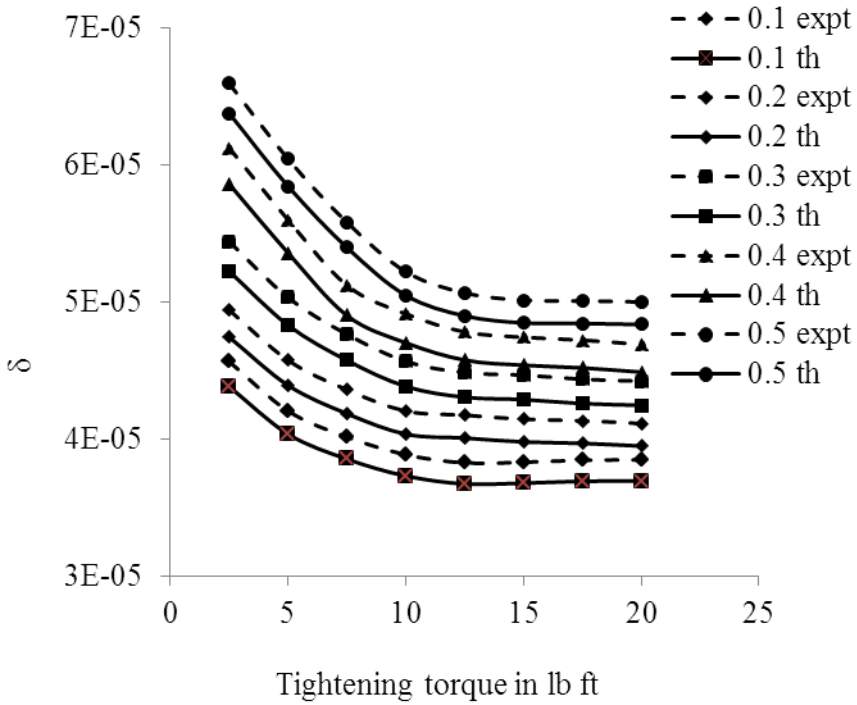

Fig.5.1 Variation of logarithmic decrement with applied tightening torque of (2+2)×49.2 mm cross-section beam with length 393.6 mm at different amplitude of excitation with thickness ratio 1.0 for non-uniform pressure at the interface.

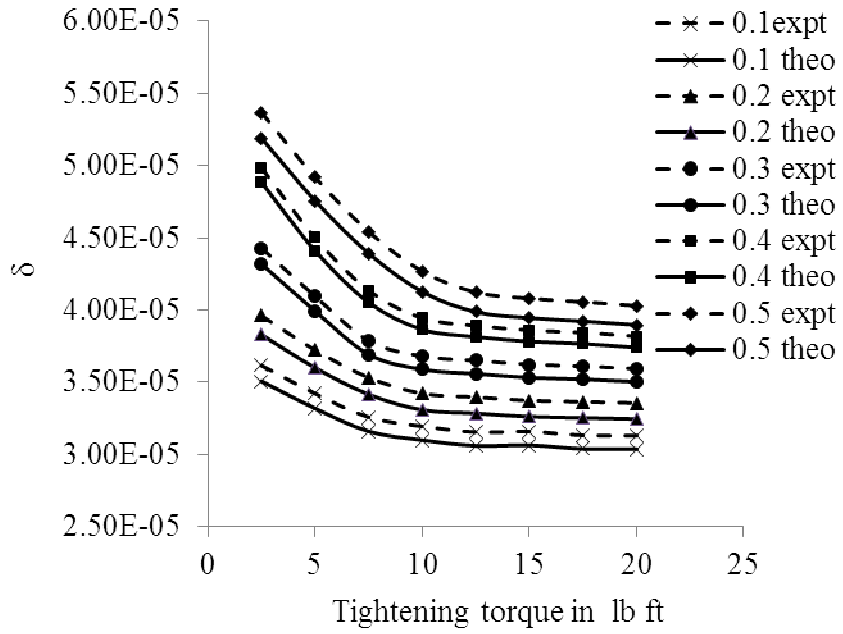

Fig.5.2 Variation of logarithmic decrement with applied tightening torque of (2+3)×57.6 mm cross-section beam with length 460.8 mm at different amplitude of excitation with thickness ratio 1.5 for non-uniform pressure at the interface.

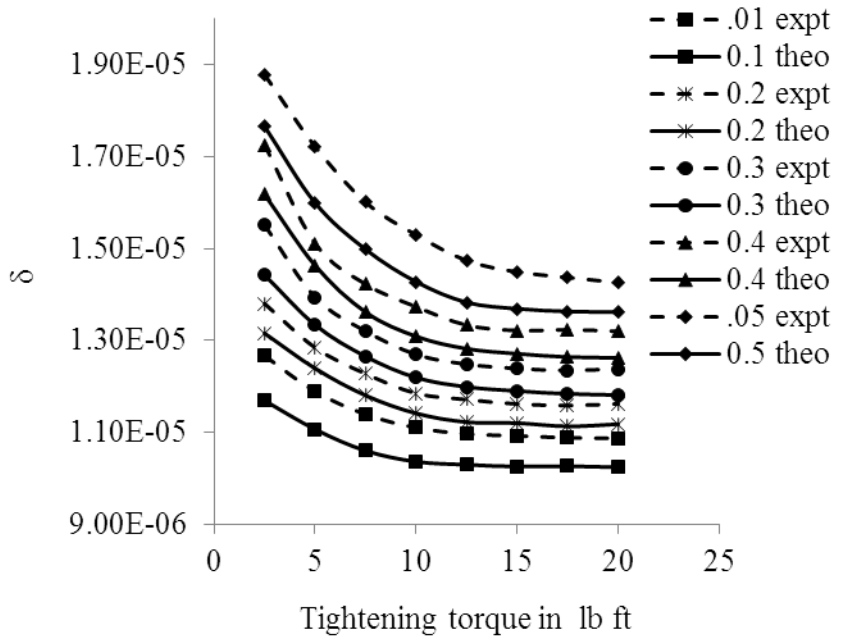

Fig.5.3 Variation of logarithmic decrement with applied tightening torque of (2+4)×66 mm cross-section beam with length 462 mm at different amplitude of excitation with thickness ratio 2.0 for non-uniform pressure at the interface.

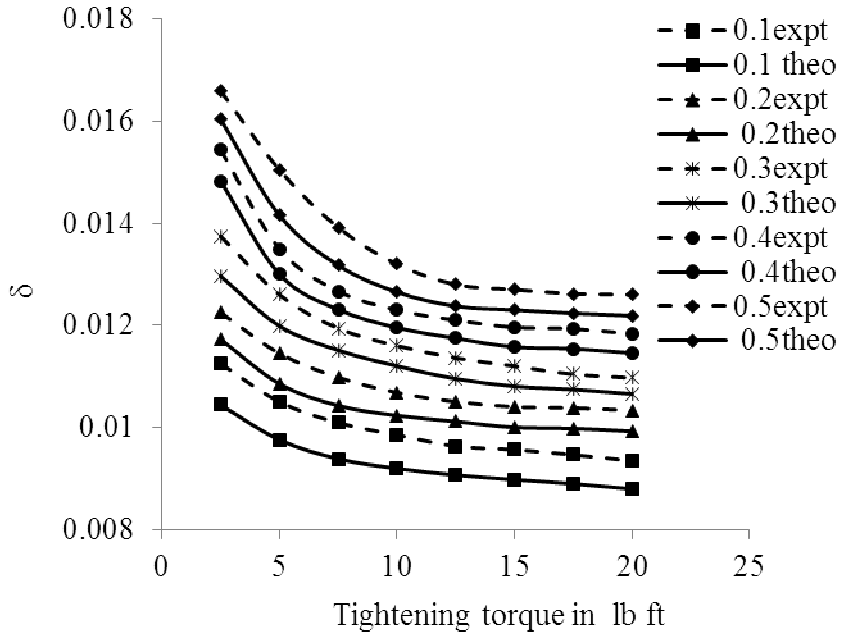

Fig.5.4 Variation of logarithmic decrement with applied tightening torque of (3+3)×28.032 mm cross-section beam with length 364.416 mm at different amplitude of excitation with thickness ratio 1.0 for uniform pressure at the interface.

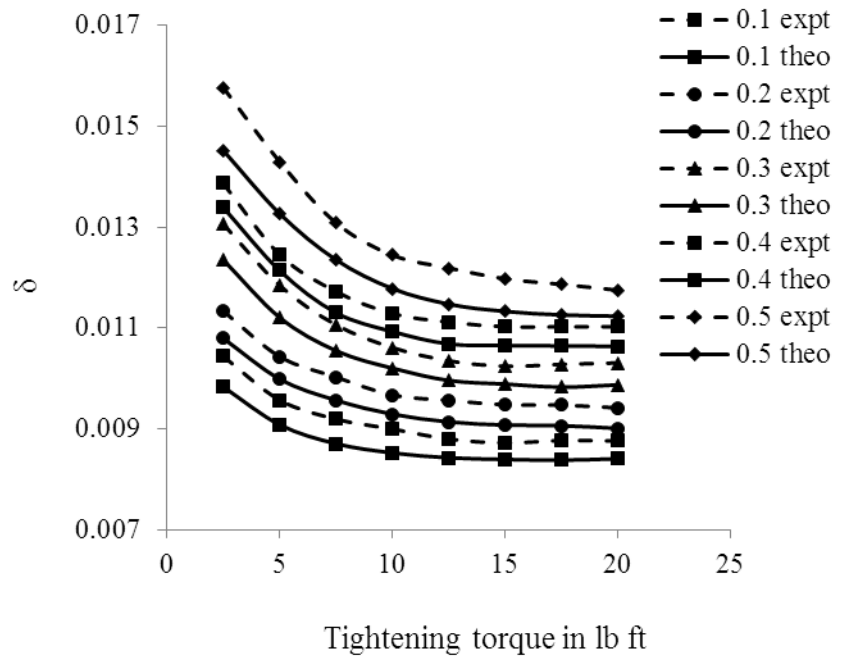

Fig.5.5 Variation of logarithmic decrement with applied tightening torque of (2+3)×28.812 mm cross-section beam with length 374.556 mm at different amplitude of excitation with thickness ratio 1.5 for uniform pressure at the interface.

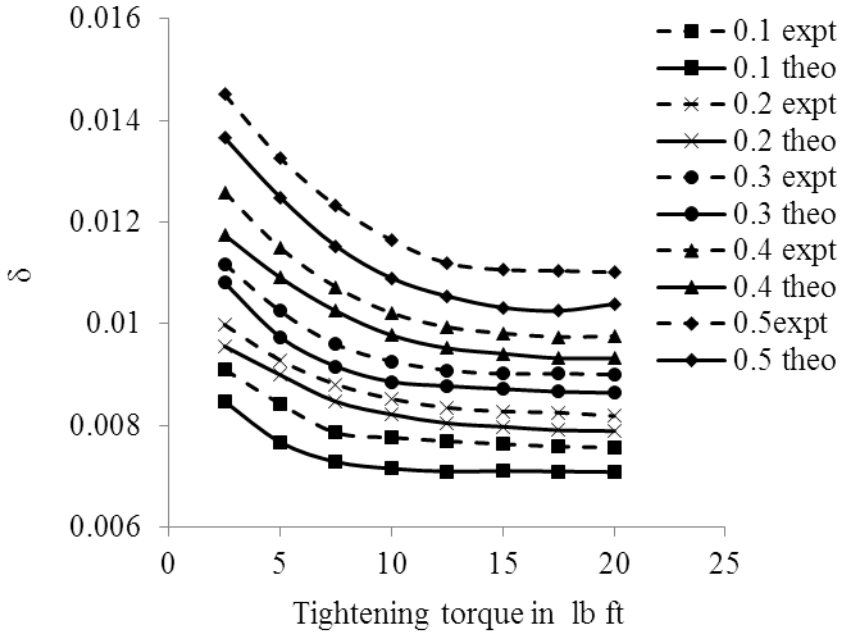

Fig.5.6 Variation of logarithmic decrement with applied tightening torque of (3+6)×28.92 mm cross-section beam with length 375.96 mm at different amplitude of excitation with thickness ratio 2.0 for uniform pressure at the interface.

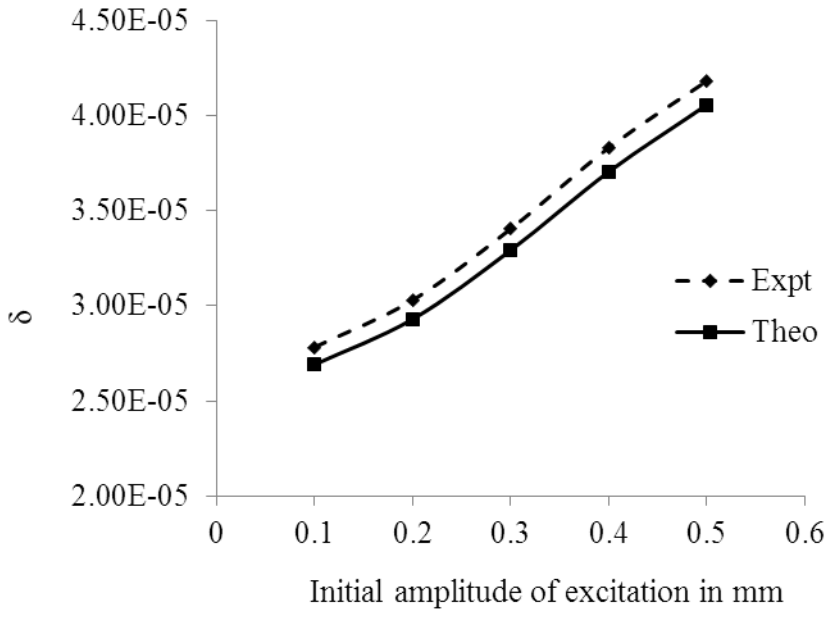

Fig.5.7 Variation of logarithmic decrement with initial amplitude of excitation for mild steel specimen of thickness ratio 1.0 for non-uniform interface pressure with beam length 344.4 mm and thickness (3+3)×49.2 mm having bolt diameter 12 mm at 2.5 lb ft tightening torque.

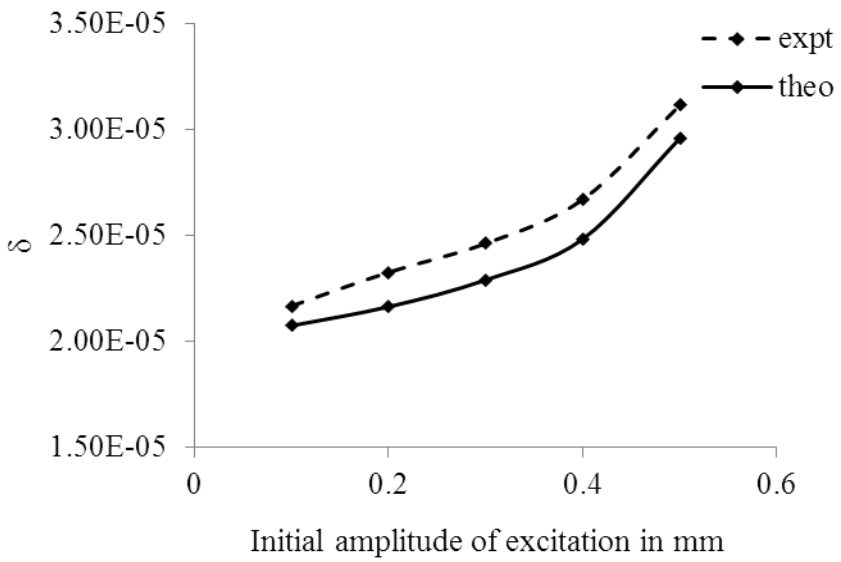

Fig.5.8 Variation of logarithmic decrement with initial amplitude of excitation for mild steel specimen of thickness ratio 1.5 for non-uniform interface pressure with beam length 403.2 mm and thickness (3+4.5)×57.6 mm having bolt diameter 12 mm at 5 lb ft tightening torque

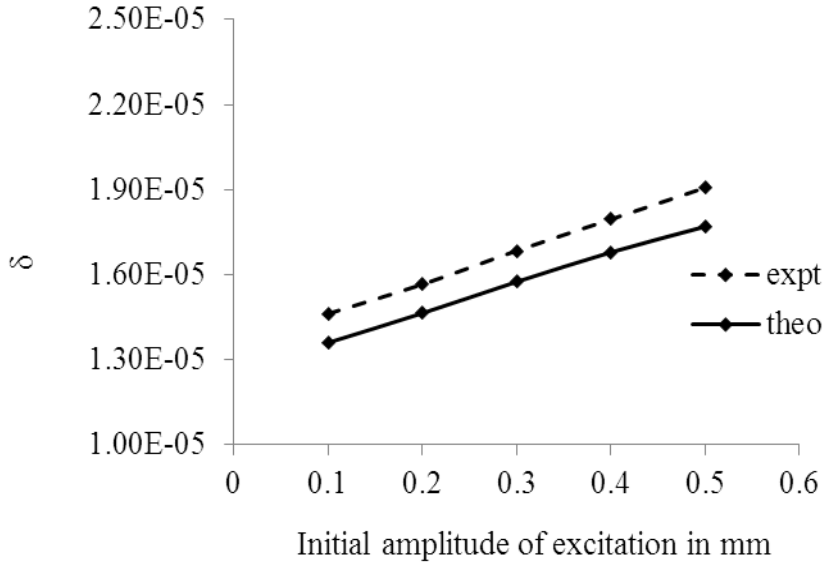

Fig.5.9 Variation of logarithmic decrement with initial amplitude of excitation for mild steel specimen of thickness ratio 2.0 for non-uniform interface pressure with beam length 528 mm and thickness (2+4)×66 mm having bolt diameter 12 mm at 10 lb ft tightening torque

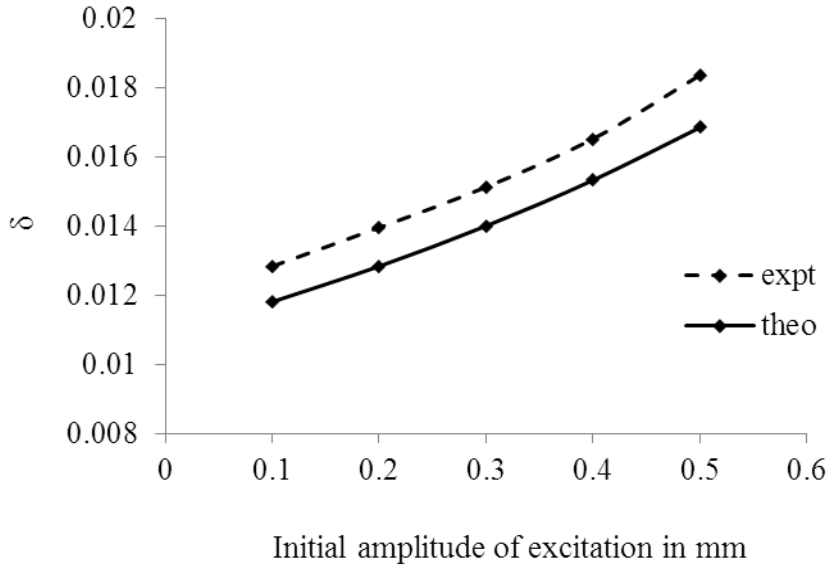

Fig.5.10 Variation of logarithmic decrement with initial amplitude of excitation for mild steel specimen of thickness ratio 1.0 for uniform interface pressure with beam length 364.416 mm and thickness (2+2)×28.032 mm having bolt diameter 12 mm at 5 lb ft tightening torque

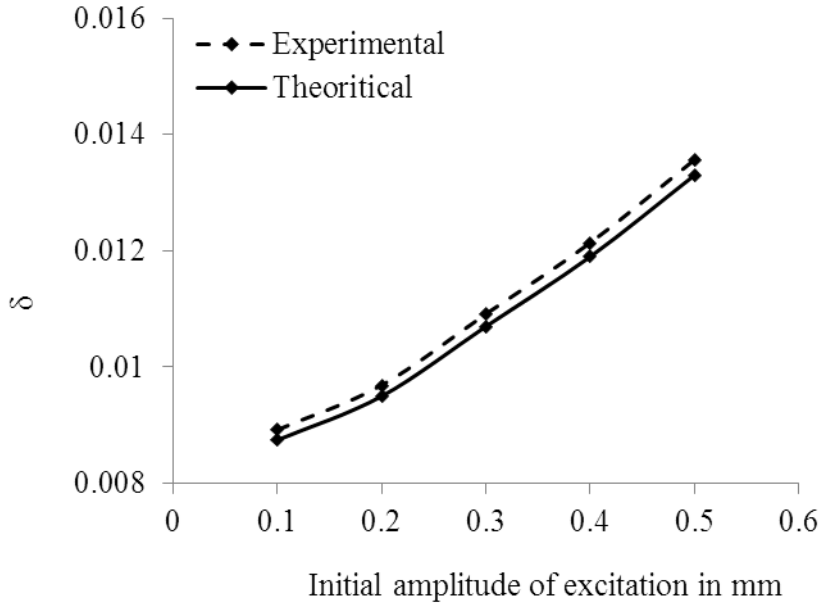

Fig.5.11 Variation of logarithmic decrement with initial amplitude of excitation for mild steel specimen of thickness ratio 1.5 for uniform interface pressure with beam length 374.556 mm and thickness (3+4.5)×28.812 mm having bolt diameter 12 mm at 5 lb ft tightening torque

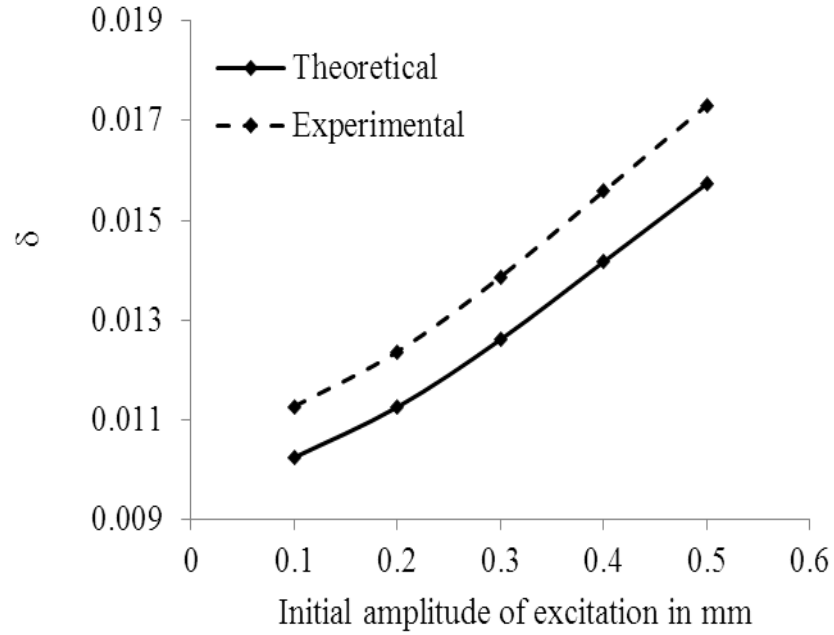

Fig.5.12 Variation of logarithmic decrement with initial amplitude of excitation for mild steel specimen of thickness ratio 2.0 for uniform interface pressure with beam length 375.96 mm and thickness (2+4)×28.92 mm having bolt diameter 12 mm at 2.5 lb ft tightening torque

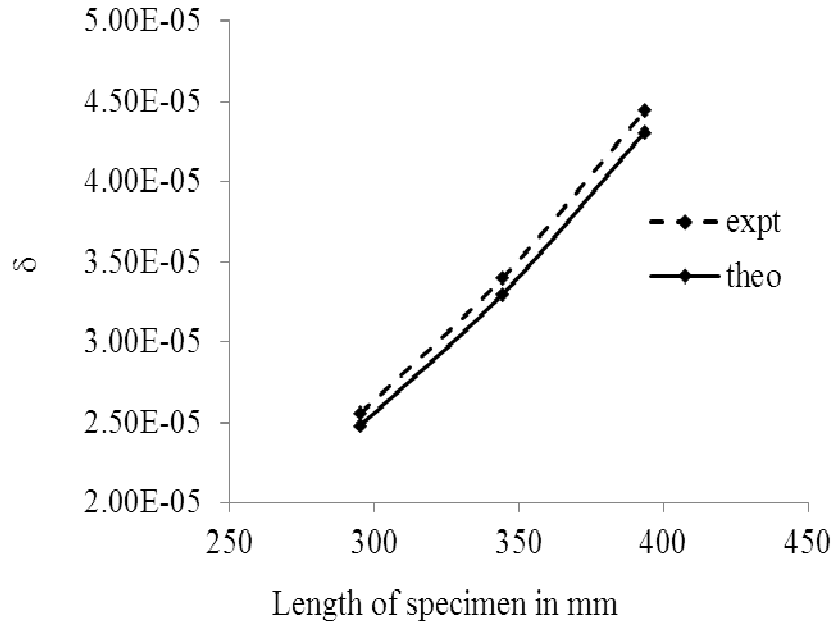

Fig.5.13 Variation of logarithmic decrement with length of mild steel specimens of cross-section (3+3)×49.2 mm at 0.3 amplitude of excitation with thickness ratio 1.0 for non-uniform interface pressure at 2.5 lb ft tightening torque

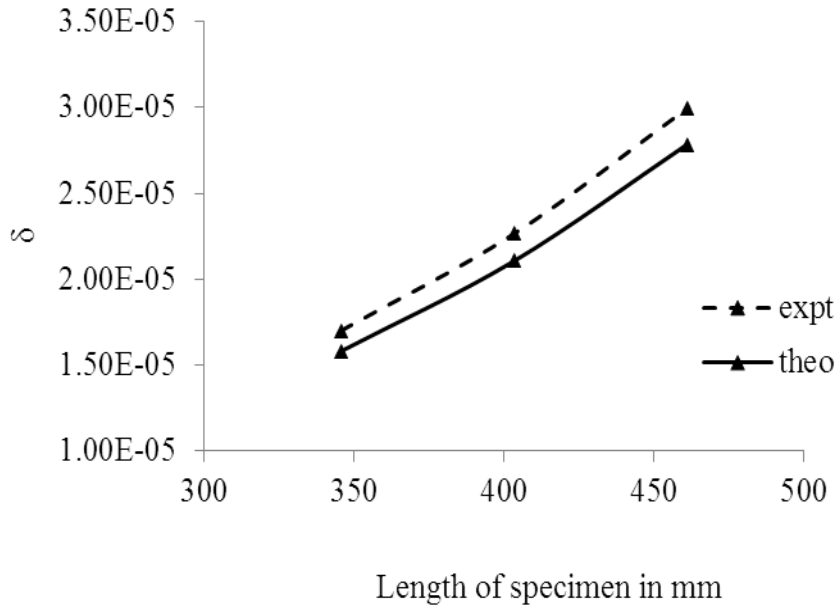

Fig.5.14 Variation of logarithmic decrement with length of mild steel specimens of cross-section (3+4.5)×57.6 mm at 0.1 amplitude of excitation with thickness ratio 1.5 for non-uniform interface pressure at 2.5 lb ft tightening torque

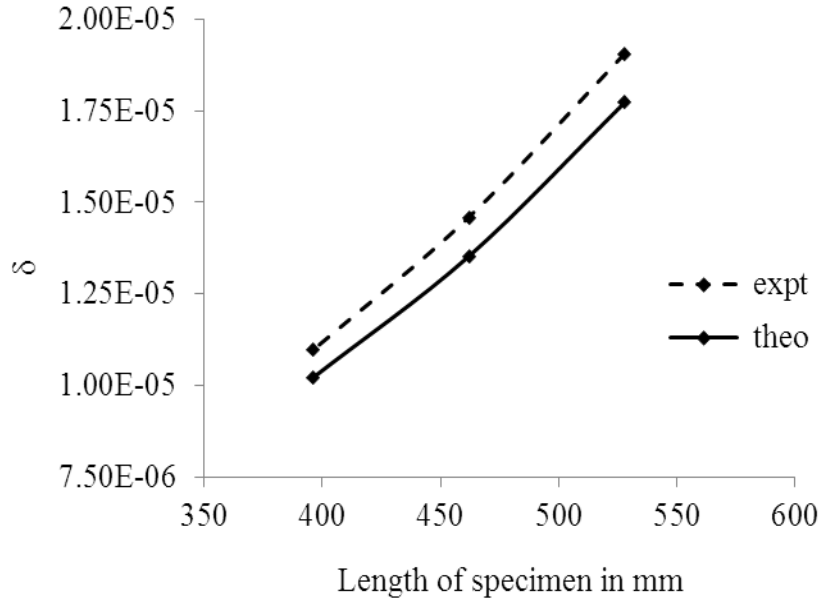

Fig.5.15 Variation of logarithmic decrement with length of mild steel specimens of cross-section (2+4)×66 mm at 0.5 amplitude of excitation with thickness ratio 2.0 for non-uniform interface pressure at 10 lb ft tightening torque

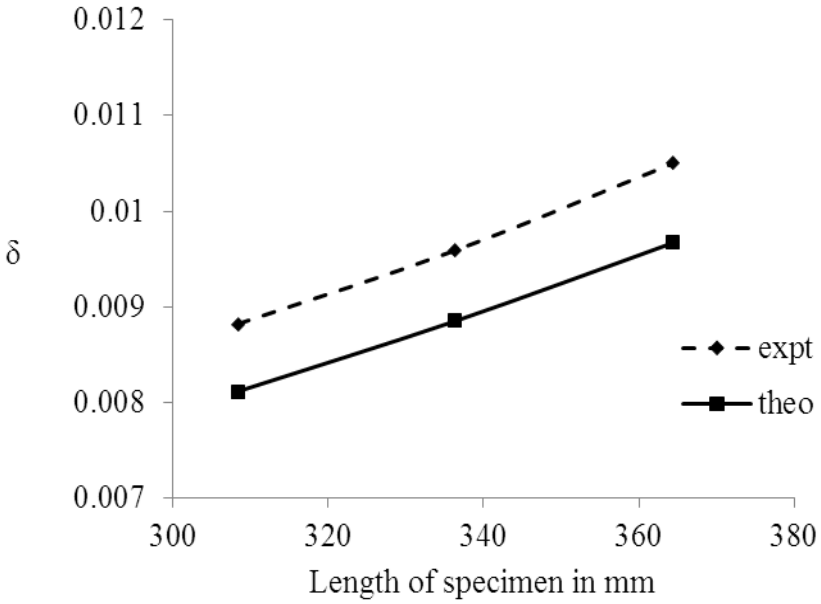

Fig.5.16 Variation of logarithmic decrement with length of mild steel specimens of cross-section (3+3)×28.032 mm at 0.1 amplitude of excitation with thickness ratio 1.0 for uniform interface pressure at 5 lb ft tightening torque

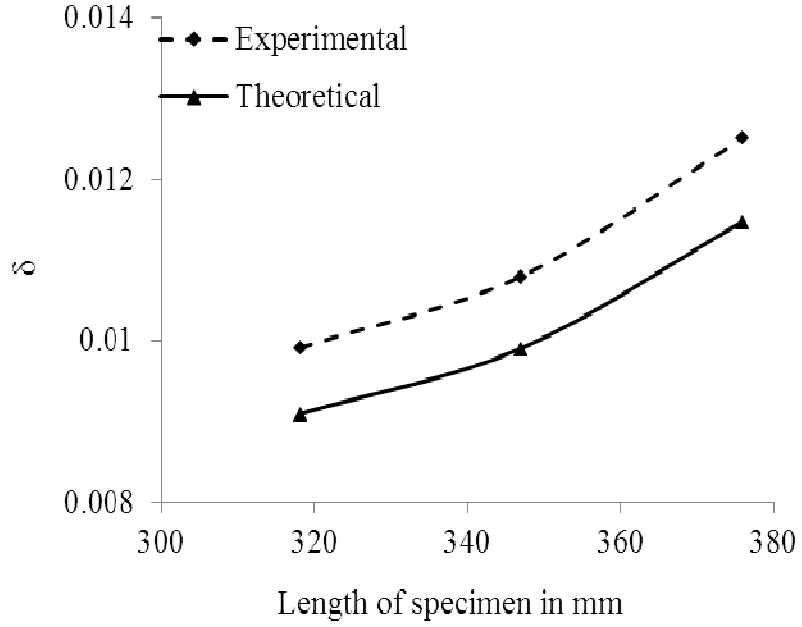

Fig.5.17 Variation of logarithmic decrement with length of mild steel specimens of cross-section (2+3)×28.812 mm at 0.1 amplitude of excitation with thickness ratio 1.5 for uniform interface pressure at 2.5 lb ft tightening torque

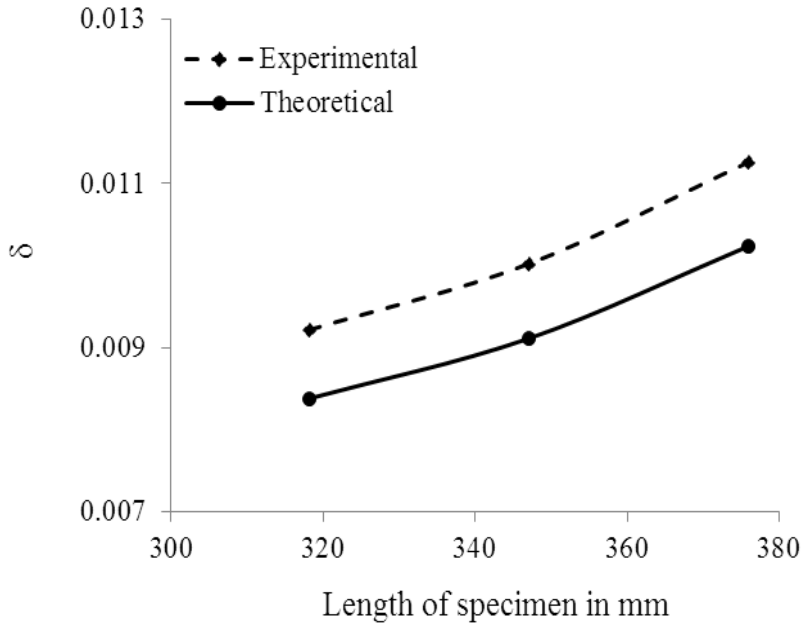

Fig.5.18 Variation of logarithmic decrement with length of mild steel specimens of cross-section (2+4)×28.92 mm at 0.1 amplitude of excitation with thickness ratio 2.0 for uniform interface pressure at 2.5 lb ft tightening torque

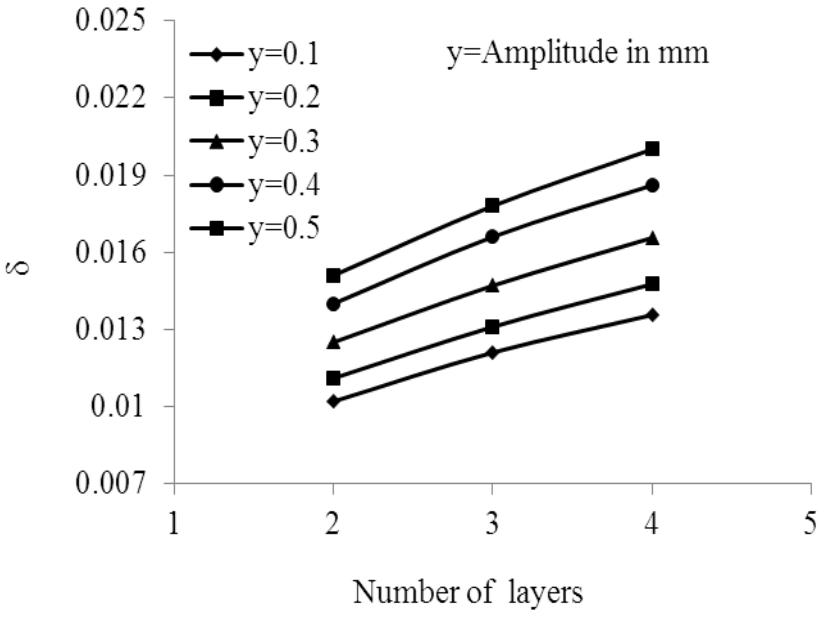

Fig.5.19 Variation of logarithmic decrement with number of layers for uniform interface pressure with thickness 2h=2 mm and length of beam is 364.416 mm of thickness ratio 1.0

From the theoretical analysis and experimental results the following salient points have been observed as detailed below.

1. It is established that the interface pressure distribution between the contacting layers jointed by connecting bolts is not uniform but parabolic in nature being maximum at the surface of the bolt hole and gradually decreases towards the circumference. The distance between the consecutive bolts is 4.10, 4.8 and 5.5 times of the diameter of bolt for thickness ratio 1.0, 1.5 and 2.0 respectively for non-uniform pressure distribution. For attaining uniform pressure distribution at the interface the adjoining interface pressure distributions are superimposed by reducing the distance between the consecutive bolts. The optimum distance is found out using MATLAB software as 2.336, 2.401 and 2.410 times the diameter of the bolts for thickness ratios of 1.0, 1.5 and 2.0 respectively. Due to excitation, relative motion, termed as micro-slip, occurs at the interfaces of the connecting members. The energy dissipation depends on the dynamic slip and friction force and is greatly influenced by the interface pressure distribution at the contact surfaces around a connecting bolt.
2. The logarithmic damping decrement decreases with increase in tightening torque on the connecting bolts as evident from the Fig 5.1 to Fig 5.6. The increase in tightening torque increases the axial load on the bolt and reduces the relative dynamic slip at the interfaces, thereby tending the jointed beam to behave like a solid one. Although the normal force at the interfaces increases, the net effect is a decrease in the logarithmic damping decrement of the layered and jointed beam because of reduced dynamic slip at the interfaces.
3. The logarithmic damping decrement increases with increase in initial amplitude of excitation as evident from Fig 5.7 to Fig 5.12. The increase in amplitude of excitation enhances the dynamic slip ratio at the interfaces. Although the strain energy introduced in to the system increases, the net effect is an increase in the logarithmic damping decrement of the jointed cantilever beam due to higher slip at the interfaces.
4. The length of the beam is another vital parameter that affects the damping capacity of the structures. The logarithmic damping decrement increases with an increase in length of the beam specimen as shown in Fig 5.13 to Fig 5.18. The increase in cantilever length reduces the static bending stiffness ($k = 3EI/l^3$) and

also the strain energy introduced into the system, thereby increasing the damping capacity of the layered and jointed cantilever beams.

5. The logarithmic damping decrement decreases with increase in frequency of vibration as shown in Fig 4.8 to Fig 4.13. The product of μα increases with the increase in frequency of vibration but the input strain energy increases due to higher strain energy input. The increase in frequency of vibration is associated with the enhancement of static bending stiffness [$f = (1/2\pi)\ (k/m)^{1/2}$] which enhances the input strain energy into the system, thereby reduces the logarithmic damping decrement.
6. The logarithmic damping decrement decreases with increase in thickness ratio of the beam as shown in Fig 5.7 to Fig 5.18. As the interfacial pressure distribution influencing the damping capacity changes with thickness ratio, the damping capacity of the cantilever beams changes accordingly. The lower thickness ratio contributes more damping capacity to the structures.
7. The stiffness of a jointed beam reduces with the incorporation of joints and layers. It is observed that the ratio of the stiffness of a jointed beam to that of an identical solid one is always less than one. The stiffness ratio has been calculated by carrying out the static deflection tests and is found to be decreasing with the increase in number of layers. The damping capacity of multilayered and jointed beams is more due to enhanced frictional energy loss and reduced input strain energy as shown in Fig 5.19.
8. The interface pressure between the contacting layers jointed by connecting bolts is not uniform but parabolic in nature being maximum at the surface of the bolt hole and gradually reduces towards the circumference. The optimum distance between the consecutive bolts for attaining uniform intensity of interface pressure distribution has also been found out. The damping capacity of the layered and jointed cantilever beams with uniform interface pressure is more than the beams of non-uniform pressure distribution due to higher interface pressure. For example, the logarithmic decrement for uniform pressure distribution beam is found to be 285% more compared to non-uniform pressure beam for a particular case. Therefore, the uniformly distributed beams contribute more damping compared to that of the non-uniform beams.

CHAPTER-6

CONCLUSIONS AND SCOPE FOR FURTHER RESEARCH WORK

The aim of the present research work is to estimate and improve the damping capacity of layered and jointed bolted structures. The theoretical and experimental analyses have been carried out in chapters 3 and 4 respectively. Further, the results are discussed in chapter-5 for both non-uniform and uniform interface pressure. The present chapter summarizes the important conclusions drawn from the theoretical analysis and experimental results.

Conclusion

As established, the damping capacity of the dynamically loaded structures mainly depends upon the joints or fasteners present in the structure. The maximum energy dissipation takes place due to the friction and the micro-slip at the interfaces. The damping of jointed bolted structures has been studied theoretically considering the energy approach due to friction and the dynamic slip at the contacting layers. Further, the theoretical results obtained have been authenticated by conducting extensive experiments. From the discussions elaborated in the previous chapter, it is found that the damping of layered and bolted structures can be enhanced by the appropriate selection of the following influencing parameters: (a) tightening torque on each bolt, (b) amplitude of excitation, (c) length of specimens, (d) natural frequency, (e) thickness ratio, and (f) thickness of beam specimen, etc. Finally, useful conclusions have been drawn from both the theoretical and experimental results as presented below.

The damping capacity of a layered bolted beam increases with:

- Decrease in tightening torque.
- Increase in initial amplitude of excitation.
- Increase in length of the beam.
- Decrease in frequency of vibration.
- Decrease in thickness ratio.
- Increase in numbers of layer.

It is estimated from the present investigation that the maximum variation of experimental results with the corresponding values from the classical results is 10.46%

for mild steel specimens. This establishes the authenticity of the theory developed and the techniques used for evaluating the logarithmic decrement in layered and jointed structures. This design concept can be effectively used by the manufacturers to fabricate the layered structures jointed with bolts in real applications such as in aerospace, machine structures, construction of bridges, locomotives, etc. depending upon the damping requirements.

Scope for Further Research

The present work is based on estimating the damping capacity of layered and jointed bolted structures with various thickness ratios. Moreover, the various vital parameters affecting the damping characteristics of layered and jointed bolted structures have been discussed in details. However, the present study can be extended for further research as pointed out below.

- Timoshenko beam theory can be used for analysis of logarithmic decrement instead of using Euler-Bernoulli beam theory.
- The same analysis can be used for other boundary conditions such as fixed-fixed, fixed-supported, supported-supported, etc.
- Forced vibration or higher modes of vibration can be used in the analysis.
- Frequency domain (FRF) analysis can be employed.
- The same can be used for layered and jointed beams of dissimilar materials.

Reference

1. Asoor, A. A. A. and Pashaei, M. H. (2010), “Experimental study on the effects of type of joint on damping”. World applied sciences Journal, Vol. 8(5), pp. 608-613.
2. Beards, C. F. and Williams, J. L. (1977), “The damping of structural vibration by rotational slip in joints”. Journal of Sound and Vibration, Vol. 53(3), pp. 333-340.
3. Beards, C. F. (1982), “Damping in structural joints”. The Shock and Vibration Digest, Vol. 14, pp. 9–11.
4. Beards, C. F. (1983), “The damping of structural vibration by controlled interface slip in joints”. ASME, Journal of Vibration, Acoustics, Stress and Reliability and in Design, Vol. 105 (3), pp. 369–373.
5. Beards, C. F. (1992), “Damping in structural joints”. The Shock and Vibration Digest, Vol. 24(7), pp. 3-7.
6. Bradly, T. L. (1968), “Stress analysis for thermal contact resistance across bolted joints”. M. S. Thesis. Massachusetts, Institute of Technology, Cambridge, MA.
7. Clarence, W. de Silva (2000), “Vibration: Fundamentals and Practice”. CRC Press LLC, Boca Raton.
8. Clarence, W. de Silva (2007), “Vibration Damping, Control, and Design”. CRC Press, Taylor and Francis Group LLC, Boca Raton.
9. Cochardt, A. W. (1954), “A method for determining the internal damping of machine members”. ASME, Journal of Applied Mechanics, Vol. 76(9), pp. 257-262.
10. Damisa, O. Olunloyo, V. O. S. Osheku, C. A. and Oyediran, A. A. (2007), “Static analysis of slip damping with clamped laminated beams”. European Journal of Scientific Research, Vol. 17(4), pp. 455-476.
11. Damisa, O. Olunloyo, V. O. S. Osheku, C. A. and Oyediran, A. A. (2008), “Dynamic analysis of slip damping in clamped layered beams with non-uniform pressure distribution at the interface”. Journal of Sound and Vibration, Vol. 309, pp. 349-374.
12. Den Hartog, J. P. (1931), “Forced vibrations with combined coulomb and viscous friction”. Transactions of the ASME, Vol. 53(9), pp. 107-115.

13. EL-Zahry R. M. (1985), “Investigation of the vibration behaviour of pre-loaded bolted joints”. Dirasat-Eng. Technology, Vol. 12, 201-223.
14. Fernlund, I. (1961), “Method to calculate the pressure between bolted or riveted plates”. Transactions of Chalmers University of Technology, Gothenberg, Sweden, Vol. 245.
15. Gaul, L. and Lenz, J. (1997), “Nonlinear dynamics of structures assembled by bolted joints”. Acta Mechanica, Vol. 125, 169-181.
16. Gaul, L. and Nitsche, R. (2000), “Friction control for vibration suppression”. Mechanical Systems and Signal Processing, Vol. 14(2), pp. 139-150.
17. Gaul, L. and Nitsche, R. (2001), “The role of friction in mechanical joints”. ASME, Applied Mechanics Reviews, Vol. 54(2), pp. 93-106.
18. Goodman, L. E. Klumpp, J. H. (1956), “Analysis of slip damping with reference to turbine blade vibration”. Journal of Applied Mechanics, Vol. 23, pp. 421.
19. Gould, H. H. and Mikic B. B. (1972), “Areas of contact and pressure distribution in bolted joints”. Transactions of ASME. Journal of Engineering for Industry, Vol. 94(3), pp. 864-870.
20. Greenwood, J. A. (1964), “The elastic stress produced in the mid plane at a slab by pressure applied symmetrically at its surface”. Proceedings of the Cambridge Philosophical Society, Cambridge, Vol. 60, pp. 159-169.
21. Groper, M. (1985), “Micro-slip and macro-slip in bolted joints”. Experimental Mechanics, June, pp.171-174.
22. Hanks, B. R. and Stephens, D. G. (1967), “Mechanisms and scaling of damping in a practical structural joint”. Shock and Vibration Bulletin, Vol. 36, pp. 1–8.
23. Hansen, S. W. and Spies, R. D. (1997), “Structural damping in laminated beams due to interfacial slip”. Journal of Sound and Vibration, Vol. 204(2), pp. 183-202.
24. Irving, E. Sumner, Raymond, F. Lacovic, and Andrew, J. Stofan, (1966), “Experimental investigation of liquid sloshing in a scale model centaur liquid-hydrogen tank”. NASA, Lewis Research Center, Cleveland, Ohio, July-7, 891-01 -00-06-22.
25. Jezequel, L. (1983), “Structural damping by slip in joints”. ASME, Journal of Vibration, Acoustics Stress, Reliability and Design, Vol. 105(2), pp. 497–504.

26. Kobayashi, T. and Matsubayashi, T. (1986), “Considerations on the improvement of the stiffness of bolted joints in machine tools”. Transactions of the Japan Society of Mechanical Engineering, Vol. 52, pp. 1092-1096.
27. Lardner, T. J. (1965), “Stresses in a thick plate with axially symmetric loading”. Transactions of ASME, Journal of Applied Mechanics, Vol. 32, pp. 458-459.
28. Marshall, M. B., Lewis, R. and Dwyer-Joyce, R. S., (2006), “Characterization of contact pressure distribution in bolted joints”, Strain, Vol. 42(1), pp. 31-43.
29. Masuko, M. Ito, Y. and Yoshida, K. (1973), “Theoretical analysis for a damping ratio of a jointed cantibeam”. Bulletin of JSME, Vol. 16(99), pp. 1421-1432.
30. Menq, C. H. Bielak, J. and Griffin, J. H. (1996), “The influence of micro-slip on vibratory response. Part-I: A new micro slip model”. Journal of Sound and Vibration, Vol. 107(2), pp. 279-293.
31. Minakuchi, Y. Koizumi, T. Shibuya, T. (1985), “Contact pressure measurement by means of ultrasonic waves using angle probes”. Bulletin of JSME, Vol. 28(243), pp. 1859-1863.
32. Minakuchi, Y. Yoshimine, K. Koizumi, T. and Hagiwara, T. (1985), “Contact pressure measurement by means of ultrasonic waves: On a method of quantitative measurement”. Bulletin of JSME, Vol. 28(235), pp. 40-45.
33. Mohanty, R. C. and Nanda, B. K. (2009), “Damping in layered and jointed riveted structures with equal thickness”. Journal of Mechanical Engineering Science, Vol. 223, pp. 319-327.
34. Motosh, M. (1975), “Stress distribution in joints of bolted or riveted connections”. Transactions of ASME. Journal of Engineering for Industry, Vol. 97(1), pp. 157-161.
35. Murty, A. S. R. and Padmanabhan, K. K. (1982), “Effect of surface topography on damping in machine joints”. Precision Engineering, Vol. 4, pp. 185-190.
36. Nanda, B. K. and Behera, A. K. (1999), “Study on damping in layered and jointed structures with uniform pressure distribution at the interfaces”. Journal of sound and vibration, Vol. 226(4), pp. 607-624.
37. Nanda, B. K. (2006), “Study of the effect of bolt diameter and washer on damping in layered and jointed structures”. Journal of Sound and Vibration, Vol. 290, pp. 1290-1314.

38. Nishiwaki, N. Masuko, M. Ito, Y. and Okumura, I. (1980), "A study on damping capacity of a jointed cantilever beam". 2nd Report: Comparison between theoretical and experimental values, Bulletin of JSME, Vol. 23(177), pp. 469-475.
39. Nishiwaki, N. Masuko, M. Ito, Y. and Okumura, I. (1978), "A study on damping capacity of a jointed cantilever beam (1st report; experimental results)". Bulletin of JSME, Vol. 21, pp. 524-531.
40. Olofsson, U. and Hagman, L. (1997), "A model for micro-slip between flat surfaces based on deformation of ellipsoidal elastic bodies", Tribology International, Vol. 30(8), pp. 599-603.
41. Olunloyo, V. O. S. Damisa, O. Osheku, C. A. and Oyediran, A. A. (2007), "Further results on static analysis of slip damping with clamped laminated beams". European Journal of Scientific Research, Vol. 17(4), pp. 491-508.
42. Sextro, W. (2002), "Dynamical contact problems with friction: Models, methods, experiments and applications". Lecture notes in Applied Mechanics, Series editor, Pfeiffer, F., Springer. Vol. 3.
43. Shigley, J. E. Mischke, R. and Brown, T. H. Jr. (2004), "Standard Handbook of Machine Design". Third Edition. Mc-Graw Hill Book Company.
44. Shin, Y. S. Iverson, J. C. and Kim, K. S. (1991), "Experimental studies on damping characteristics of bolted joints for plates and shells". Transactions of ASME, Journal of Pressure Vessel Technology, Vol. 113(3), pp. 402-408.
45. Sidorov, O. T. (1983), "Change of the damping of vibrations in the course of operation in dependence on the parameters of bolted joints". Strength of Materials, Vol. 14, pp. 671-674.
46. Song, S. Park, C. Moran, K. P. and Lee, S. (1992), "Contact area of bolted joint interface". Analytical, finite element modeling and experimental study. ASME EEP. ASME, Vol. 3, pp. 73-81.
47. Thomson, W. T. (1993), "Theory of Vibration with Applications". 2nd Edition, George Allen and Unwin, London.
48. Tsai, J. S. and Chou, Y. F. (1988), "Modeling of the dynamic characteristics of two-bolted joints". Journal of Chinese Institute of Engineering, Vol. 11, pp. 235-245.

49. Ungar, E.E. (1973), “The status of engineering knowledge concerning the damping of built-up structures”. Journal of Sound and Vibration, Vol. 26, pp. 141-154.
50. Ziada, H. H. and Abd, A. K. (1980), “Load pressure distribution and contact areas in bolted joints”. Institution of Engineers (India), Vol. 61, pp. 93-100.

Curriculum Vitae

Name: ARUNDHATI PRADHAN

E-mail: arudhati.pradhan@gmail.com

Date of birth: 1st July 1981

Nationality: Indian

Permanent Address: Qrs. No-N/38, H.A.L. TOWNSHIP, Sunabeda, Dist: Koraput

PIN: 763002, State- Odisha,

India

Education: Bachelor Degree in Mechanical Engineering,

Institute-G.I.E.T., Gunupur (India), 2006

Publications

- International journal:
  1. "Investigation of damping mechanism in layered and bolted beams with unequal thickness ratio and uniform pressure distribution at the interfaces", International journal of applied engineering research, ISSN 0973-4562 Volume 6, Number 5 (2011) pp.711-718.
- International conference:
  1. "Damping mechanism in layered beams of unequal thickness ratio with uniform pressure distribution at the interfaces", 5th International Conference on Advances in Mechanical Engineering (ICAME-2011), 06-08, June 2011, S. V. National Institute of Technology, Surat, India.
  2. "Mechanism of slip damping in layered bolted cantilever beams with varying thickness ratio", International conference on modeling optimisation and computing (ICMOC -2012), 10-11, April 2012, NI University, Kumaracoil, Nagercoil, Tamilnadu, India.
  3. "Damping mechanisms of layered bolted cantilever beams with non-uniform pressure at the interfaces and unequal thickness ratio", Accepted for

presentation in First World Congress on Advances in Structural Engineering and Mechanics (ASEM'11plus), Seoul, Korea.

- National conference:

1. "Investigation of damping mechanism in layered and bolted beams with uniform pressure distribution at the interfaces", National Conference on Emerging Research and Advances in Mechanical Sciences (ERA-2011), 23rd March 2011, Velammal Engineering College, Chennai, India.

2. "Investigation of damping mechanism in layered and bolted beams with unequal thickness ratio and uniform pressure distribution at the interfaces", National Conference on Design and Manufacturing (NaConDM2011) 27-28, May 2011, Indian institute of information technology design and manufacturing (iiitd&m) Kancheepuram, Chennai, India.

3. **"**Damping mechanism in layered bolted cantilever beams with varying thickness ratio", National Conference on "Recent Advances in Mechanics and Materials (RAMM-2012) 25-26, February 2012, Veer Surendra Sai University of Technology, Burla, Odisha, India**.**